In vivo analysis of NH_4^+ transport and central nitrogen metabolism in Saccharomyces cerevisiae during aerobic nitrogen-limited growth

Cueto-Rojas, H. F.; Maleki Seifar, R.; ten Pierick, A.; van Helmond, W.; Pieterse, M. M.; Heijnen, J. J.; Wahl, S. A.

DOI
10.1128/AEM.01547-16

Publication date
2016

Document Version
Final published version

Published in
Applied and Environmental Microbiology

AMERICAN SOCIETY FOR MICROBIOLOGY | Applied and Environmental Microbiology

In Vivo Analysis of NH_4^+ Transport and Central Nitrogen Metabolism in *Saccharomyces cerevisiae* during Aerobic Nitrogen-Limited Growth

H. F. Cueto-Rojas, R. Maleki Seifar, A. ten Pierick, W. van Helmond, M. M. Pieterse, J. J. Heijnen, S. A. Wahl

Cell Systems Engineering Group, Department of Biotechnology, Delft University of Technology, Delft, The Netherlands

ABSTRACT

Ammonium is the most common N source for yeast fermentations. Although its transport and assimilation mechanisms are well documented, there have been only a few attempts to measure the *in vivo* intracellular concentration of ammonium and assess its impact on gene expression. Using an isotope dilution mass spectrometry (IDMS)-based method, we were able to measure the intracellular ammonium concentration in N-limited aerobic chemostat cultivations using three different N sources (ammonium, urea, and glutamate) at the same growth rate (0.05 h^{-1}). The experimental results suggest that, at this growth rate, a similar concentration of intracellular (IC) ammonium, about 3.6 mmol NH_4^+/$liter_{IC}$, is required to supply the reactions in the central N metabolism, independent of the N source. Based on the experimental results and different assumptions, the vacuolar and cytosolic ammonium concentrations were estimated. Furthermore, we identified a futile cycle caused by NH_3 leakage into the extracellular space, which can cost up to 30% of the ATP production of the cell under N-limited conditions, and a futile redox cycle between Gdh1 and Gdh2 reactions. Finally, using shotgun proteomics with protein expression determined relative to a labeled reference, differences between the various environmental conditions were identified and correlated with previously identified N compound-sensing mechanisms.

IMPORTANCE

In our work, we studied central N metabolism using quantitative approaches. First, intracellular ammonium was measured under different N sources. The results suggest that *Saccharomyces cerevisiae* cells maintain a constant NH_4^+ concentration (around 3 mmol NH_4^+/$liter_{IC}$), independent of the applied nitrogen source. We hypothesize that this amount of intracellular ammonium is required to obtain sufficient thermodynamic driving force. Furthermore, our calculations based on thermodynamic analysis of the transport mechanisms of ammonium suggest that ammonium is not equally distributed, indicating a high degree of compartmentalization in the vacuole. Additionally, metabolomic analysis results were used to calculate the thermodynamic driving forces in the central N metabolism reactions, revealing that the main reactions in the central N metabolism are far from equilibrium. Using proteomics approaches, we were able to identify major changes, not only in N metabolism, but also in C metabolism and regulation.

Saccharomyces cerevisiae is a versatile organism that can grow on a large variety of N sources, namely, ammonium (NH_4^+), urea, citrulline, ornithine, gamma aminobutyric acid (GABA), allatoin, allantoate, and all proteinogenic L-amino acids, with the exceptions of L-lysine, L-histidine, and L-cysteine (1, 2). Therefore, *S. cerevisiae* cells require complex machinery to achieve metabolic regulation for efficient uptake and anabolic and catabolic processing of N compounds.

In particular, *S. cerevisiae* can differentiate between preferred and nonpreferred N sources using the nitrogen catabolite repression (NCR) pathway. This system allows yeast cells to first use N sources that promote a high growth rate, such as ammonium and glutamine, in preference to compounds that sustain low growth rates, such as isoleucine and methionine (1–3). Although nitrogen-sensing mechanisms have still not been completely elucidated, several regulatory proteins, including Ure2, Gln3, Gzf3, Tor1, Tor2, and Dal80, are known to influence the expression of NCR-sensitive genes.

One of the most relevant preferred N sources for *S. cerevisiae* is ammonia/ammonium, which is the second most common N compound on earth and a common N source for many organisms from the three kingdoms of life (4, 5). In aqueous solution, ammonia (NH_3) is protonated, producing the ammonium (NH_4^+) ion (equation 1).

$$NH_{4(aq)}^{+} \overset{pK_a = 9.25}{\longleftrightarrow} NH_{3(aq)} + H_{(aq)}^{+} \quad (1)$$

The sum of both species, NH_3 and NH_4^+, is referred to below as total ammonium. It is widely accepted that NH_3 can diffuse through cell membranes, with a permeability coefficient of 48 × 10^{-3} cm/s (1.73 m/h) in synthetic bilayer lipid membranes (6) and

Received 3 July 2016 **Accepted** 8 September 2016

Accepted manuscript posted online 16 September 2016

Citation Cueto-Rojas HF, Maleki Seifar R, ten Pierick A, van Helmond W, Pieterse MM, Heijnen JJ, Wahl SA. 2016. *In vivo* analysis of NH_4^+ transport and central nitrogen metabolism in *Saccharomyces cerevisiae* during aerobic nitrogen-limited growth. Appl Environ Microbiol 82:6831–6845. doi:10.1128/AEM.01547-16.

Editor: D. Cullen, USDA Forest Products Laboratory

Address correspondence to S. A. Wahl, s.a.wahl@tudelft.nl, or H. F. Cueto-Rojas, H.F.CuetoRojas@gmail.com.

Supplemental material for this article may be found at http://dx.doi.org/10.1128/AEM.01547-16.

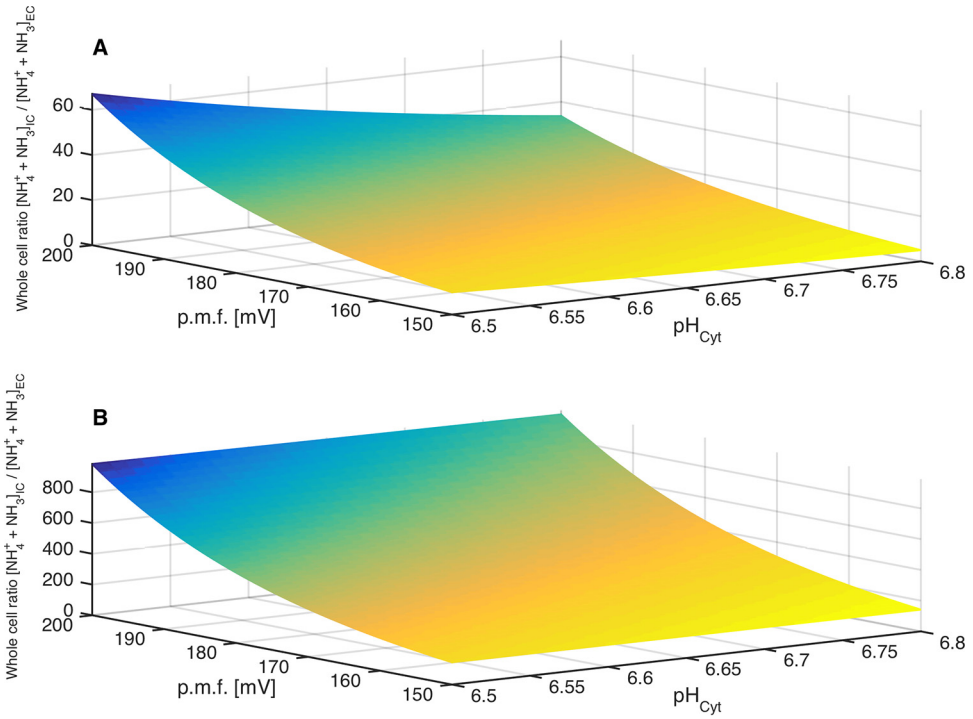

FIG 1 Thermodynamic equilibrium whole-cell (IC)/EC ratios of the ammonium transporter—if a uniport mechanism is considered—at different values of pH_{Cyt} and PMF. (A) Values if it is assumed that ammonium is evenly distributed in the whole cell (no compartmentalization). (B) NH_3 diffusion from the cytosol into an acidic compartment (vacuole) significantly increases the IC/EC ratios. Whole-cell concentrations were calculated using the intracellular mass balance for ammonium (equation 8), NH_3 diffusion between the cytosol and the vacuole is considered to be an equilibrium process; the cytosol/vacuole ratio was calculated using equation 9. The following assumptions were made: $pH_{Vac} = 4.5$, $V_{Cyt} = 0.7\ V_{Cell}$, $V_{Vac} = 0.14\ V_{Cell}$, and $pH_{EC} = 5$.

53×10^{-3} cm/s (1.91 m/h) in erythrocyte membranes (7). In contrast, there is an ongoing debate about the particularities of the protein-mediated transport mechanism for NH_4^+ (8–11). In particular, in *S. cerevisiae*, Mep proteins (methylamine and ammonium permeases) are responsible for ammonium transport (12) and sensing (13). The available experimental evidence (14, 15) suggests that ammonium is transported against the NH_3 concentration gradient but in favor of an electrochemical gradient, meaning that the mechanism must be membrane potential driven (4, 16). The three known Mep proteins are Mep1p, Mep2p, and Mep3p, with reported K_m values of 5 to 10 μM, 1 to 2 μM, and 1.4 to 2.1 mM, respectively (17).

Assuming that ammonium is transported via a uniport mechanism dependent on the electrochemical gradient of ammonium ions across the cell membrane (16), it is possible to calculate the cytosolic/extracellular (Cyt/EC) ratio of total ammonium at thermodynamic equilibrium using equation 2 (a full derivation of the equation is shown in Fig. S1 in the supplemental material).

$$\frac{\left[NH_3 + NH_4^+\right]_{total,Cyt}}{\left[NH_3 + NH_4^+\right]_{total,EC}} = \left(\frac{1 + 10^{pH_{Cyt}-pK_a}}{1 + 10^{pH_{EC}-pK_a}}\right) \times \exp\left(\frac{z \times F \times \Delta\psi_m}{R \times T}\right) \quad (2)$$

Under common cultivation conditions for *S. cerevisiae* (pH_{EC} = 5; temperature [T] = 303 K) with a cytosolic pH (pH_{Cyt}) of 6.5, the membrane potential ($\Delta\psi_m$) is equal to 110 mV (with the inside negative), and the proton motive force value (PMF) is equal to 200 mV (inside negative). The maximum Cyt/EC ratio of total ammonium then equals 67, which indicates that the intracellular (IC) ammonium concentration is higher than in the extracellular space (Fig. 1). Thus, it is clear that the electrochemically driven Mep-dependent mechanism is advantageous for *S. cerevisiae* to transport and accumulate intracellular ammonium, particularly when ammonium concentrations are low, which is typically the case in grape juice (18) and other ecologically relevant environments for *S. cerevisiae*, such as fruit juices and fermentation musts, which are rich in fermentable sugars (19).

Urea is another industrially relevant nitrogen source for *S. cerevisiae* cultivations, particularly due to its safety, low cost, and high availability. Urea can be transported into the intracellular space using either (i) passive diffusion/facilitated uniport uptake at urea concentrations above 0.5 mmol urea/liter (20) or (ii) an H^+ symport protein (Dur3) with an apparent K_m of 14 μmol/liter (20) when extracellular concentrations of urea are lower than 0.25 mmol/liter (21). In the intracellular space, urea is metabolized via an ATP-dependent urea amidolyase (Dur1,2) (22), producing two molecules of ammonia and one molecule of CO_2 at the cost of the hydrolysis of one ATP molecule. Although urea can sustain a high growth rate, similar to ammonium conditions, it is a nonrepressive N source; as such, NCR-controlled genes are not repressed. Furthermore, the SPS sensor of extracellular amino acids is not activated (3). Consequently, urea is one of the most interesting N sources for the study of nitrogen-controlled metabolism. Glutamate is another preferred N source, which is imported through a specific transporter. Several genome scale stoichiometric models

consider that the transport mechanism is a Glu^-/H^+ symport (23–25); the thermodynamic equilibrium Cyt/EC ratio of this mechanism at pH 5 can be calculated to be around 28 (see Fig. S1 in the supplemental material). It is known that amino acids promote the expression of their own specific transporters; for instance, several amino acids trigger the response of the SPS-sensing mechanism that leads to the expression of certain amino acid permeases (1, 2). Glutamate in particular, being the central point of N metabolism, is expected to affect the expression of proteins related to C and N metabolism.

In the cytosol of *S. cerevisiae*, glutamate and glutamine are used to produce other amino acids. Nevertheless, all N sources are converted into free ammonium, particularly for the production of glutamine if it is not present in the medium. Ammonium is assimilated using two main pathways to produce glutamate and glutamine. The first pathway involves the enzyme glutamate dehydrogenase (Gdh) NADPH dependent (equation 3), which uses 2-oxo-glutarate (αKG) as the substrate.

$$NH_4^+ + NADPH + \alpha KG \xrightarrow{Gdh} \text{L-glutamate} + H_2O + NADP \quad \Delta_r G^{0'} = -30.5\ \text{kJ/mol} \quad (3)$$

The second pathway is catalyzed by two enzymes, glutamine synthase (equation 4) and glutamine 2-oxo-glutarate amino transferase (equation 5); this pathway is also called the GS-GOGAT system (equation 6). The amino group from glutamate is reported to be the source of 80% of the cellular nitrogen (26), with the amido group from glutamine being the source of the remaining 20% (26).

$$NH_4^+ + ATP + \text{L-glutamate} \xrightarrow{GS} \text{L-glutamine} + ADP + Pi + H^+ \quad \Delta_r G^{0'} = -5.6\ \text{kJ/mol} \quad (4)$$

$$NADH + \alpha KG + \text{L-glutamine} + H^+ \xrightarrow{GOGAT} 2 \times \text{L-glutamate} + NAD^+ \quad \Delta_r G^{0'} = -56.2\ \text{kJ/mol} \quad (5)$$

$$NH_4^+ + NADH + \alpha KG + ATP \xrightarrow{GS-GOGAT} \text{L-glutamate} + ADP + Pi + NAD^+ \quad \Delta_r G^{0'} = -61.8\ \text{kJ/mol} \quad (6)$$

Comparing equations 6 and 3 shows that the GS-GOGAT system differs from Gdh by using NADH instead of NADPH, with concomitant consumption of one ATP molecule. Although the transporters and reactions by which ammonium and other N sources are assimilated in the cell are well known, the impact of the intracellular ammonium concentration on the regulatory machinery of *S. cerevisiae* is still unclear. For *S. cerevisiae*, many studies have described how central nitrogen metabolism is tightly regulated by the presence of ammonium, glutamate, glutamine, and other nitrogenous compounds (1, 27–29). It has been shown that a pulse of ammonium leads to significant changes in the expression of its own transporters and genes related to N assimilation and central carbon metabolism, among others (28).

The aim of this work was to study *in vivo* the transport and central N metabolism of *S. cerevisiae* for different N sources under aerobic N-limited conditions and the role of NH_4^+ in the transport and central N metabolism of *S. cerevisiae*, focusing particularly on the effects of the N source on the intracellular ammonium concentration and the expression levels of different proteins. The methods already available for the quantification of glutamate and glutamine (30), together with new isotope dilution mass spectrometry (IDMS)-based methods for ammonium (31) and urea, were applied to study, for three N sources (NH_4^+, urea, and glutamate), compartmentalization and the thermodynamic status of central N metabolism. Furthermore, a large proteomic survey was carried out to obtain data to elucidate the potential effects of these three N sources on protein expression. The experiments were performed with *S. cerevisiae* in aerobic chemostats, using glucose as the C source under N source limitation to avoid excessive extracellular N sources; to facilitate the study of N source transport; and, more specifically, to increase the accuracy of the intracellular NH_4^+ quantification.

MATERIALS AND METHODS

Strain and culture conditions. The prototrophic strain *S. cerevisiae* CEN.PK 113-7D was obtained from the Centraalbureau voor Schimmelcultures (Fungal Biodiversity Center, Utrecht, The Netherlands) and was cultivated in aerobic glucose-fed N-limited chemostats (dilution rate $[D] \approx 0.05\ h^{-1}$) using three different nitrogen sources: ammonium, urea, and L-glutamic acid. The media used for inoculum preparation and for batch and chemostat experiments were modifications of the N-limiting medium reported by Boer et al. (32). The medium contained 130 g/liter glucose monohydrate (656.56 mM), 1.14 g/liter $MgSO_4 \cdot 7H_2O$ (4.62 mM), 6.9 g/liter KH_2PO_4 (50.7 mM), 2 ml/liter trace elements, 2 ml/liter vitamin solution, and 0.3 g/liter antifoam C. At a low dilution rate under aerobic N-limiting conditions, metabolic oscillations (33) were observed, which are detrimental to steady-state studies. It was found empirically that supplementation of the medium with ethanol (as suggested by Suarez-Mendez et al. [34]) to a final concentration of 25 g/liter (543.48 mM) avoided these metabolic oscillations; thus, all the media contained that ethanol concentration. The N sources used were $NH_4H_2PO_4$ (3.48 g/liter), urea (0.9 g/liter), and L-glutamic acid (4.44 g/liter). All the N sources were added to a final concentration of 30.26 mmol N/liter, which is sufficient to produce about 8 g cell dry weight (g_{CDW})/liter. All media were adjusted before use to a final pH of 5 using KOH as a titrant.

To start the NH_4^+-limited culture, two 500-ml Erlenmeyer flasks containing 200 ml of ammonium-limited medium each were inoculated with 1-ml cryovials (glycerol; −80°C) of yeast cells and incubated at 30°C and 200 rpm for 12 h. After morphological inspection to check the purity of the culture, one of the flasks was used to inoculate a 7-liter bioreactor (Applikon, Schiedam, The Netherlands) with a working volume of 4 liters. The reactor temperature was kept constant at 30°C; the dissolved oxygen tension (DOT) was monitored in line using an oxygen probe (Mettler-Toledo, Tiel, The Netherlands). A stirring speed of 500 rpm, overpressure of 3×10^4 Pa, and an aeration rate of 0.5 vol/vol/min (vvm) were used to keep the dissolved oxygen level above 80%. The fractions of CO_2 and O_2 in the dry off-gas were measured on line using a combined paramagnetic-infrared analyzer (NGA 2000; Fisher-Rosemount, Hasselroth, Germany). The pH was kept at 5 with automatic additions of 4 M KOH or 2 M H_2SO_4.

Once the batch phase was finished, fresh ammonium-limited medium was fed to the reactor at a dilution rate of ~0.05 h^{-1}. After reaching steady state and taking the samples, the medium was switched to urea-limited medium, keeping the dilution rate constant; the same operation was performed to switch the N source from urea to L-glutamic acid.

All samples were taken at each steady state after stable values of DOT and off-gas CO_2 and O_2 were obtained, between three and seven volume changes after switching the medium. To obtain biomass-specific uptake and production rates, extracellular concentration measurements, flow rates, and volumes were used, together with the appropriate fermentor balance equations for broth components (glucose, ammonium, biomass, ethanol, glycerol, and acetate) and for gas components (O_2, CO_2, and ethanol). Ethanol evaporation has a large impact on the ethanol balance and C recovery; the ethanol evaporation constant (k_{evap}) was experimentally determined (see Fig. S2 in the supplemental material).

Internal standards. (i) Ammonium. Since our in-house-prepared U-^{13}C-labeled yeast cell extract contained a high concentration of $^{14}NH_4^+$, samples for intracellular ammonium quantification were prepared separately using as the internal standard a solution of $^{15}NH_4Cl$ (98 atom% ^{15}N; lot number TA0525V; Sigma-Aldrich) dissolved in Milli-Q water to a concentration of 500 μmol/liter.

(ii) Urea. [^{13}C, $^{15}N_2$]urea (99 atom% ^{13}C, 98 atom% ^{15}N; lot number SZ0618V; Sigma-Aldrich) was dissolved in Milli-Q water and added to the in-house-prepared uniformly ^{13}C-labeled yeast cell extract to a final concentration in the sample of 20 μmol/liter (the concentration in the extract equaled 100 μmol/liter). Previously, it was experimentally observed that this cell extract did not contain any labeled or nonlabeled urea; the mixture of U-^{13}C-labeled yeast cell extract and [^{13}C, $^{15}N_2$]urea was used as an internal standard in samples selected for analysis of intracellular metabolites and urea.

Sampling and sample preparation. (i) Samples for extracellular metabolites and ammonium analysis. Samples of approximately 1 ml of broth for quantification of extracellular metabolites and ammonium were quenched using cold steel beads in a syringe, as described by Mashego et al. (35), and filtered using 0.45-μm disc filters (Millipore). The filtrate (80 μl) was mixed with 20 μl of internal standard (500 μmol/liter $^{15}NH_4Cl$) and derivatized according to the protocol used for ammonium quantification by liquid chromatography-mass spectrometry (LC-MS). The rest of the filtrate was stored at −80°C until further analysis of the extracellular metabolites.

(ii) Rapid sampling and biomass extraction for intracellular metabolites and intracellular ammonium. Samples of approximately 1.2 g of broth were taken with a dedicated rapid-sampling setup (36) and quenched in 6 ml of −40°C methanol (100%), and after weighing to determine the mass of the sample, they were centrifuged for 5 min at 10,000 × *g* and −19°C. For biomass washing, the pellet was recovered and resuspended in 6 ml −40°C methanol (100%) and centrifuged again for 5 min at 10,000 × *g* and −19°C.

(iii) Cold nonbuffered chloroform-methanol (CM) extraction of the biomass pellet. The biomass pellet obtained from rapid sampling for intracellular metabolites and intracellular ammonium was recovered, and 3.5 ml of methanol–Milli-Q water (50% [vol/vol]) prechilled at −40°C was added, followed by 120 μl of U-^{13}C-labeled cell extract with labeled urea. Afterward, 3.5 ml of chloroform (100%) prechilled at −40°C was added in order to extract intracellular metabolites according to the method of Canelas et al. (37). This method was used to extract intracellular metabolites, excluding ammonium, particularly to protect acid-unstable metabolites, e.g., NADH and NADPH.

(iv) Cold chloroform-methanol buffered at pH 5 (CM5) extraction of the biomass pellet. The biomass pellet obtained from rapid sampling for intracellular metabolites and intracellular ammonium was recovered, 3.5 ml of 10 mM methanol-acetate buffer (pH 5) (50% [vol/vol]) prechilled at −40°C was added, and then 120 μl of U-^{13}C-labeled cell extract with labeled urea (intracellular metabolite samples) or 120 μl of $^{15}NH_4Cl$ (500 μmol/liter) (intracellular ammonium samples) was added as an internal standard. Afterward, 3.5 ml of chloroform (100%) prechilled at −40°C was added in order to extract intracellular metabolites according to the method of Cueto-Rojas et al. (31). Samples for quantification of intracellular ammonium were extracted using this method exclusively.

Analytical methods. (i) Dry weight, cell count, size distribution, and average cell volume. Determination of cell dry weight was performed gravimetrically using preweighted 0.45-μm filters (Millipore). The broth was removed by filtration, and the cell pellet in the filter was washed with Milli-Q water. The filters were dried at 70°C until a constant weight was reached (approximately 72 h).

To calculate the intracellular concentrations (millimoles per liter IC) from the intracellular amounts (micromoles per gram CDW), the cell volume was measured as described by Bisschops et al. (38) using a Coulter counter with a 50-μm orifice (Multisizer II; Beckman, Fullerton, CA); the average cell volume (in milliliters IC per gram CDW) was estimated using equation 7.

$$V_{cell}\left(\frac{ml_{IC}}{g_{CDW}}\right) = \frac{\text{average particle volume (fl)} \times \text{average number of particles (particles/liter)}}{\text{dry weight } (g_{CDW}/\text{liter})} \times 10^{-12} \quad (7)$$

(ii) Metabolite quantification (other than ammonium). One hundred microliters of extracellular samples was used to quantify glucose, ethanol, glycerol, and acetate using high-performance liquid chromatography (HPLC) as described by Cruz et al. (39). Quantification of αKG, pyruvate, and trehalose was performed using gas chromatography-tandem MS (GC–MS-MS) as described by Niedenfuhr et al. (40). The concentrations of the coenzymes NAD, NADH, NADP, and NADPH were measured using LC–MS-MS as described by Maleki Seifar et al. (41) and nucleotides according to the method of Maleki Seifar et al. (42). Amino acids and urea were measured using GC-MS according to the method of de Jonge et al. (30). Finally, intra- and extracellular ammonium levels were quantified according to the mehod of Cueto-Rojas et al. (31).

(iii) Protein quantification. U-^{13}C-labeled *S. cerevisiae* biomass was prepared as described by Wu et al. (43) and used as an internal standard for relative protein quantification. Cell suspensions of the sample biomass and internal standard were mixed 1:1 based on the optical density at 600 nm (OD_{600}), washed with Milli-Q water, and freeze-dried. Proteins were extracted by grinding the freeze-dried biomass with a pestle and mortar and were precooled with liquid nitrogen. After grinding, 2 ml of 50 mM phosphate-buffered saline (PBS) with 200 mM NaOH was added to extract proteins. The soluble-protein fraction was separated from the cell debris by centrifugation at 13,300 rpm for 15 min. The proteins were precipitated overnight in cold acetone at −20°C by adding 4 parts cold acetone to 1 part protein solution. After washing and drying, the protein pellet was dissolved in 400 μl of 100 mM ammonium bicarbonate (ABC) with 6 M urea. Of this solution, 20 μl was further processed; proteins were reduced by addition of tris(2-carboxyethyl)phosphine (TCEP) to a final concentration of 10 mM and incubating for 60 min at room temperature. The proteins were alkylated by addition of iodoacetamide (IAM) to a final concentration of 10 mM and incubating for 60 min at room temperature. Prior to digestion, the protein solution was 6-fold diluted by addition of 100 μl of 100 mM ABC to dilute the urea concentration to 1 M. The proteins were digested by addition of trypsin (trypsin singles, proteomics grade; Sigma-Aldrich) at a 1:100 ratio and incubating at 37°C for 16 h. The digested protein mixture was purified and concentrated using an in-house-made solid-phase-extraction (SPE) pipette tip with 5-μm particles of Reprosil-Pur C_{18}-Aq reversed-phase (RP) material (Maisch GmbH, Ammerbuch-Entringen, Germany).

Digested peptides were separated using nanoflow chromatography performed with a vented column system essentially as described by Meiring et al. (44) and a 2-dimensional precolumn (RP-strong cation exchange [SCX]-RP). Analytical columns (50-μm inside diameter [i.d.]) were prepared with a 1-mm potassium silicate (Kasil) frit and packed with 5-μm particles of Reprosil-Pur C_{18}-Aq reversed-phase material to a length of 40 cm. The capillary RP-SCX-RP precolumn (150-μm i.d.) was prepared with a 1-mm Kasil frit and packed with 5-μm particles of Reprosil-Pur C_{18}-Aq reversed-phase material to a length of 17 mm; with 5-μm particles of the strong cation exchange material Polysulfoethyl A (PolyLC, Columbia, MD, USA) for 60 mm; and again with 5-μm particles of Reprosil-Pur C_{18}-Aq reversed-phase material for 17 mm (total length, 94 mm). The different column materials were kept separate from each other by insertion of a piece of glass wool. The LC equipment and solvents used were similar to those used by Finoulst et al. (45). Each sample analysis consisted of six fractionations. In the first fractionation, the peptides were injected and trapped on the precolumn by applying 100% solvent A for 10 min. Then, a first linear gradient from 4 to 35% B in 75 min was applied. After this, a linear gradient to 80% B was followed for 6 min and then 3 min of 80% B. Finally, the column was reconditioned for 26 min

TABLE 1 Overview of the main experimental results for different N sources

Experimental variable	Value[a] for N source:		
	NH_4^+	Urea	L-Glutamate
Biomass concn (C_X) (g_{CDW}/liter)	7.4 ± 0.1	7.6 ± 0.1	7.1 ± 0.0
Residual glucose (C_S) (mmol/liter)	117.5 ± 3.6	113.1 ± 4.9	144.7 ± 2.2
Residual N source (C_N) (mmol/liter)	0.008 ± 0.002	0.024 ± 0.010	0.467 ± 0.021
μ (h^{-1})	0.0517 ± 0.0002	0.0525 ± 0.0002	0.0501 ± 0.0002
$-q_{N\ source}$ (μmol N/g_{CDW}/h)	226 ± 12	222 ± 2	223 ± 2
$-q_{O2}$ (mmol/g_{CDW}/h)	1.52 ± 0.02	1.43 ± 0.01	0.98 ± 0.01
q_{CO2} (mmol/g_{CDW}/h)	7.16 ± 0.08	7.25 ± 0.07	7.21 ± 0.03
$-q_S$ (mmol/g_{CDW}/h)	3.70 ± 0.05	3.91 ± 0.06	4.03 ± 0.02
q_{EtOH} (mmol/g_{CDW}/h)	5.00 ± 0.10	5.15 ± 0.25	5.87 ± 0.05
q_{ATP} (mmol/g_{CDW}/h)[b]	7.88 ± 0.10	7.86 ± 0.25	7.73 ± 0.05
N content (% [wt/wt])[c]	6.1 ± 0.3	5.9 ± 0.2	6.2 ± 0.0
Avg cell vol (ml_{IC}/g_{CDW})	2.13 ± 0.07	1.97 ± 0.03	1.88 ± 0.05
Intracellular trehalose (μmol/g_{CDW})	266.1 ± 5.4	249.2 ± 37.7	252.9 ± 14.9
Intracellular glutamate (μmol/g_{CDW})	83.8 ± 2.8	71.7 ± 8.2	151.2 ± 11.2
Intracellular ammonium (μmol/g_{CDW})	6.9 ± 2.3	7.4 ± 0.7	7.2 ± 2.2
Extracellular ammonium (μmol/$liter_{EC}$)	7.6 ± 0.5	7.6 ± 4.0	9.1 ± 1.4

[a] Values for experimentally measured concentrations and cell volume are averages ± standard deviations (SD) of three independent samples from the same steady state. The N contents and q rates are reported as mean values ± SD calculated assuming linear error propagation.
[b] Calculated as the sum of ATP produced through alcoholic fermentation and complete substrate oxidation. Assuming 1 mol ATP/mol ethanol and a P/O ratio of 0.95 (50), this leads to the following equation: $q_{ATP} = q_{EtOH} + 2 \times 0.95 \times -q_{O2}$.
[c] Calculated from the values of q_N and μ reported here.

with 100% A. In the following 5 fractionations, peptides were eluted by injection of 10 μl 5, 10, 50, 250, or 1,000 mM ammonium formate, pH 2.6, respectively, from the autosampler (followed by 100% A for 10 min). Again, a first linear gradient from 4 to 35% B in 75 min was applied, followed by a second linear gradient to 80% B for 6 min and then 3 min of 80% B. After each fractionation, the column was reconditioned for 26 min with 100% A. This resulted in six fractionations per sample, with a total run time of 12 h per sample. For each analysis, ~10 μg of protein was injected.

Mass spectrometry was performed using a protocol derived from that of Finoulst et al. (45). Full-scan MS spectra (from m/z 400 to 1,500; charge states 2 and higher) were acquired at a resolution of 30,000 at m/z 400 after accumulation to a target value of 10^6 ions (automatic gain control). Nine data-dependent MS-MS scans (higher-energy collisional dissociation [HCD] spectra; resolution, 7,500 at m/z 400) were acquired using the 9 most intense ions with a charge state of 2+ or higher and an ion count of 10,000 or higher. The maximum injection time was set to 500 ms for the MS scans and 200 ms for the MS-MS scan (accumulation for MS-MS was set to a target value of 5×10^4). Dynamic exclusion was applied, using a maximum-exclusion list of 50, one repeat count, a repeat duration of 10 s, and an exclusion duration of 45 s. The exclusion window was set from −10 to +10 ppm relative to the selected precursor mass.

Data processing and analysis were performed similarly to the method of Finoulst et al. (45). Briefly, MS-MS spectra were converted to Mascot generic files (MGFs) using Proteome Discoverer 1.4 (ThermoFisher Scientific) and DTASuperCharge version 2.0b1 (46). MGFs from the 6 SCX fractions of the same sample were combined using MGFcombiner version 1.10 (46). The samples were analyzed with the Mascot v2.2.02 search engine (Matrix Science, Boston, MA, USA). As the reference proteome, the Uniprot (47) proteome of *S. cerevisiae* strain ATCC 204508/288c (UniProt identifier UP000002311; 6,634 sequences) was used.

Carbamidomethyl cysteine was set as a fixed modification and oxidized methionine as a variable modification. Trypsin was specified as the proteolytic enzyme, and up to three missed cleavages were accepted. Mass tolerance for fragment ions was set at 0.05 Da and for precursor peptide ions at 10 ppm. Peptides with a Mascot score of <10 were removed, and only the highest-scoring peptide matches for each query listed under the highest-scoring protein were selected. Proteins were quantified using MSQuant version 2.0b7 (46) by importing the html file of the Mascot results with the corresponding raw mass spectrometric data files. MSQuant automatically calculated peptide and protein ratios by using a ^{13}C quantitation method (in quantitationmodes.xml) containing 7 modifications based on the number of carbon atoms each amino acid contains. The difference in mass between ^{12}C and ^{13}C is 1.00335 Da, resulting in mass shifts of 2 (glycine), 3 (ASC), 4 (NDT), 5 (EQMPV), 6 (RHILK), 9 (FY), or 11 (W) carbon atoms. Quantification was restricted to peptides with a Mascot score of ≥25.

RESULTS

Overview of the q rates found under N-limited aerobic cultivations. Table 1 shows the experimental results of the N-limited cultures, and q rates (biomass specific conversion rates) are shown for the different N sources. As expected, they were very similar, because the same growth rate was used. The residual glucose concentration was much higher than with a glucose-limited chemostat, which was 0.07 mM (34), showing that N source limitation was achieved.

There was also high ethanol production and a high trehalose content (approximately 10% [wt/wt]), which was to be expected under N source limitation (48, 49). Finally, the N source limitation was confirmed by the low extracellular concentrations of the N sources used. The N uptake rate (in micromoles of N per gram CDW per hour) was the same for each N source used and shows that the biomasses for the three N sources had N contents ranging between 5.92% and 6.23%, which was also as expected. Using the q values, it is possible to estimate the ATP production rate, assuming that 1 mol ATP is produced per mol ethanol and 1.90 mol ATP is produced per mol O_2 consumed (50); this results in almost exactly the same value of q_{ATP} (about 7.8 mmol ATP/g_{CDW}/h) for each of the three N sources. Under aerobic glucose-limited conditions, it is known that 1 mol ATP allows the synthesis of 16 g_{CDW} (51), which at a μ value (i.e., specific growth rate) of 0.05 h^{-1} results in a q_{ATP} value of 3.12 mmol ATP/g_{CDW}/h. On the other hand, under aerobic N-limited conditions, 1 mol ATP could pro-

duce 6.5 g_{CDW}. This comparison shows that, under N-limited conditions and independent of the N source, there is extra ATP dissipation of 4.7 mmol/ATP/g_{CDW}/h with respect to glucose limitation.

Intracellular and extracellular concentrations of N sources under N-limited conditions. The intracellular and extracellular NH_4^+ analysis produced surprising results. (i) NH_4^+ was transported from inside to outside when urea or glutamate was used as the N source. This was deduced from the presence of extracellular ammonium. A similar phenomenon was observed by Marini et al. (17) and Boeckstaens et al. (52). (ii) For the three N sources, the intracellular and extracellular NH_4^+ concentrations were very similar. This suggests that the NH_4^+-scavenging/uptake mechanisms have similar affinity and equilibrium constants in all cases, implying a common NH_4^+ transport mechanism. (iii) The intracellular total-ammonium concentrations for the three N sources were almost the same. Using the measured average cell volumes, the intracellular total-ammonium concentrations were 3.24, 3.76, and 3.82 mmol/$liter_{IC}$. For urea, which is hydrolyzed to ammonium and CO_2, a similar intracellular concentration was expected. For L-glutamate as the N source, we expected a lower concentration, given that nitrogen is already provided as an amino acid and ammonium is required only for L-glutamine synthesis. The nearly constant level points to an important role for intracellular NH_4^+ in the regulation of N metabolism. (iv) Under the test conditions, more than 85% of total broth ammonium was inside the cells and the remainder was found in the extracellular space. (v) The total intracellular/extracellular (IC/EC) concentration ratio of NH_4^+ was about 475 for the three N sources. This is far higher than the Cyt/EC equilibrium ratio of 67 expected for the assumed NH_4^+ uniporter. One hypothesis, elaborated below, is that there is strong compartmentalization of NH_4^+ between the cytosol and vacuole (Fig. 2).

For the urea-limited culture, the intracellular and extracellular urea concentrations showed that, in contrast with NH_4^+ as the N source, the majority (80%) of the total broth urea was found in the extracellular space. The intracellular urea concentration (151 μmol/$liter_{IC}$) was higher than the extracellular concentration (23 μmol/$liter_{EC}$), and the IC/EC ratio of 6 differs from the expectation based on urea uniport, which sets a maximum Cyt/EC ratio of 1. From the glutamate-limited culture, it follows that around 70% of the glutamate is found in the intracellular space. The IC/EC ratio is >200, also higher than the ratio of 28 expected from a Glu^-/H^+ symporter equilibrium.

Intracellular metabolites and large proteomics survey. As well as the intracellular concentrations of the N sources, different metabolites were also measured (Table 2) to determine the thermodynamic status of the most relevant reactions involved in the central N metabolism. It is particularly interesting to analyze the glutamate dehydrogenase NAPDH-dependent (Gdh1) reaction, as it is the main N-assimilating reaction in *S. cerevisiae*. Table 3 shows the most relevant N metabolism reactions under NH_4^+-, urea-, and glutamate-limiting conditions.

Finally, the experimental design was set up so that the different N sources would allow identification of the differences in expression of key proteins of the central nitrogen metabolism; in particular, it was aimed at covering a large number of proteins from the proteome of *S. cerevisiae* to identify regulators, transcription factors, and key pathway enzymes (see Fig. 4A for a summary of the main results of our proteomic survey, showing that more than 500 proteins were identified with more than 3 confidence peptides [characteristic peptides resulting from protein hydrolysis]). From this analysis, only the main findings are discussed; the bulk of the results can be found in Data Set S1 in the supplemental material.

DISCUSSION

NH_4^+ compartmentalization model of *S. cerevisiae*. From our NH_4^+ experimental results, it appears that the measured intracellular/extracellular ratio of 475 is far higher than the equilibrium value of 67 (Fig. 2) calculated for the assumed uniport mechanism. Nevertheless, the IC/EC ratio does point to a membrane potential-driven mechanism. This counters the conclusions reached by Soupene et al. (53), who suggested that Mep proteins transport NH_3. From our experimental results, it is clear that Mep proteins transport NH_4^+/NH_3 against the concentration gradient of NH_3 but in favor of an electrochemical gradient. A possible explanation for such high IC/EC ratios is the presence of an NH_4^+/H^+ symporter; it is highly unlikely that such a transporter is active in yeast. As discussed by many authors, the Mep/Amt protein family transports ammonium, probably by uniport of NH_4^+ (5, 16, 54) or a thermodynamically equivalent (14) mechanism. Currently, there is no further evidence to support the hypothesis of a symporter mechanism. An NH_4^+ symport was reported by Ritchie (55), who described an Na^+/NH_4^+ symporter mechanism in cyanobacteria at extracellular pH 7.5.

Wood et al. (15) argued that, in the cytosol of plant cells, ammonium (NH_4^+) deprotonates into ammonia (NH_3) and this uncharged species diffuses into the vacuole, where it is protonated once again due to the acidic pH of the compartment. It is reasonable to assume that a similar mechanism occurs in yeast. First, ammonia (NH_3) diffuses from the slightly acidic environment of the cytosol (pH_{Cyt} 6.5) into the much more acidic vacuolar space, with pH_{Vac} between 4 and 5 (56). If no other transporter removes ammonium from the vacuole, an equilibrium ratio of ammonium across the vacuolar membrane where $[NH_4^+]_{Vac}$ is much greater than $[NH_4^+]_{Cyt}$ can be obtained.

It has been estimated that the vacuolar volume is close to 14% of the total cell volume. On the other hand, the mitochondrial volume is around 1%, and cytosol accounts for 70% of the entire cell volume (57). Using these compartment volumes, a feasible ammonium distribution (cytosol, mitochondria, and vacuole) can be estimated. (i) The balance of intracellular ammonium and compartment volumes relative to the whole cell is given by equation 8.

$$\left[NH_3 + NH_4^+\right]_{IC} = 0.7 \times \left[NH_3 + NH_4^+\right]_{Cyt} + 0.14 \times \left[NH_3 + NH_4^+\right]_{Vac} + 0.01 \times \left[NH_3 + NH_4^+\right]_{Mit} \quad (8)$$

(ii) The ammonium vacuole/cytosol and mitochondria/cytosol equilibrium ratios can be calculated by assuming that NH_3 diffusion is the only transport mechanism between these compartments. These equilibrium ratios are dependent on the pH difference between compartments (e.g., pH_{Cyt} 6.5, pH_{Mit} 7.5, and pH_{Vac} 4.5). The vacuole is the most relevant NH_4^+ storage compartment, and the equilibration assumption of NH_3 is relevant for discussion. To calculate the NH_3 flux to the vacuole, its area is needed; assuming a large spherical vacuole per cell with a diameter of 0.77 μm (a sphere that occupies 14% of the cell volume, on average 34 fl/cell as measured in this study) results in a vacuolar area (a_{Vac}) of 0.11 m^2/g_{CDW}. From the measured intracellular NH_4^+ concentration (3.24 mmol/$liter_{IC}$) (Table 1), it is possible to

A

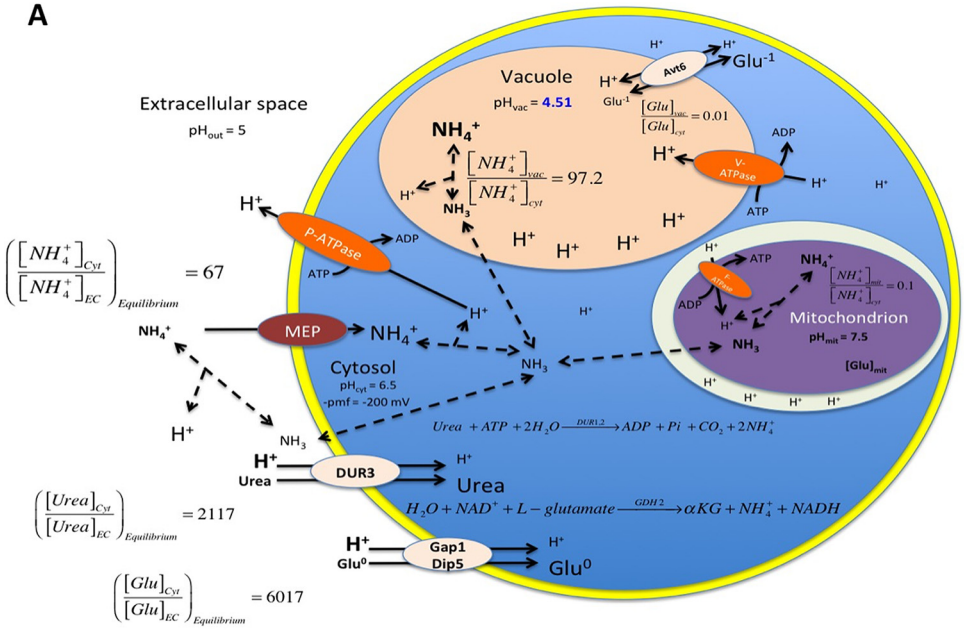

B

N-source	NH_4^+	Urea	L-glutamate
pH_{Vac}	4.51	4.51	4.51
$[NH_3+NH_4^+]_{EC}$ (μmol/L_{EC})*	7.6 ± 0.5	7.6 ± 4.0	9.1 ± 1.4
$[NH_3]_{EC}$ (μmol/L_{EC})	4 × 10^{-4}	4 × 10^{-4}	5 × 10^{-4}
$[NH_3+NH_4^+]_{IC}$ (μmol/L_{IC})*	3239 ± 1097	3755 ± 343	3820 ± 1188
$[NH_4^+]_{Cyt}$ (μmol/L_{Cyt})	226	262	267
$[NH_3]_{Cyt}$ (μmol/L_{Cyt})	0.4	0.5	0.5
$[NH_4^+]_{Vac}$ (μmol/L_{Vac})	22005	25508	25948
$[NH_4^+]_{mit}$ (μmol/L_{mit})	23	27	27
$[Urea]_{EC}$ (μmol/L_{EC})*	BQL	23.7 ± 9.9	BQL
$[Urea]_{IC}$ (μmol/L_{IC})*	BQL	151.3 ± 83.6	BQL
$[Urea]_{Cyt}$ (μmol/L_{Cyt})	BQL	216	BQL
$[L\text{-}glu]_{EC}$ (μmol/L_{EC})	BQL	BQL	467 ± 118
$[L\text{-}glu]_{IC}$ (μmol/L_{IC})*	39.4 ± 1.4 × 10^3	36.4 ± 4.2 × 10^3	80.5 ± 5.9 × 10^3
$[L\text{-}glu]_{Cyt}$ (μmol/L_{Cyt})	50.5 × 10^3	46.7 × 10^3	103 × 10^3
$[L\text{-}glu]_{Vac}$ (μmol/L_{Vac})	0.7 × 10^3	0.7 × 10^3	1.4 × 10^3
$[L\text{-}glu]_{mit}$ (μmol/L_{mit})	394 × 10^3	364 × 10^3	805 × 10^3

* Value experimentally measured
BQL = Below Quantification Limit
$[L\text{-}glu]_{mit}$ is calculated assuming that 10% of the total pool is mitochondrial, (Lu *et al.*, 2008)

FIG 2 (A) Different mechanisms proposed for ammonium, urea, and L-glutamate uptake and potential mechanisms for intracellular compartmentalization of L-glutamate and ammonium. (B) Estimated pH_{Vac} and intracellular distribution of ammonium, urea, and L-glutamate for *S. cerevisiae* growing under aerobic N-limited conditions ($D = 0.05\ h^{-1}$) using different N sources.

estimate the intracellular NH_3 at cytosolic pH (pH_{Cyt} 6.5) as 0.006 mol/m_{IC}^3. Assuming that all intracellular ammonium is cytosolic results in a maximum NH_3 flux into the vacuole of 1.2 mmol NH_3/g_{CDW}/h NH_3 $flux_{Vac} = P_{1a} \times a_{Vac} \times [NH_3]_{Cyt}$ [where P_{1a} is the permeability coefficient of ammonia $\{NH_3\}$ over the cell membrane] considering a permeability of 1.73 m/h (6). This illustrates that the maximum flux over the membrane could be more than five times higher than the N uptake rate (0.226 mmol/g_{CDW}/h) (Table 1) and shows that the cytosol/vacuole equilibrium assumption is realistic due to the potentially high NH_3 diffusion rate between the compartments. In contrast, NH_3 diffusion over the cell membrane into the cytosol is much slower due to the low extracellular pH (pH_{EC} 5) and total ammonium concentration (7.6 μmol/$liter_{EC}$) and results in very low $(NH_3)_{EC}$ concentrations and also very low NH_3 diffusion fluxes into the cytosol. (iii) The vacuolar and mitochondrial pHs are variables needed in the system of algebraic equations, but it is assumed that the cytosolic and mitochondrial pHs remain the same as previously measured in exponentially growing cells: 6.5 (58) and 7.5 (59), respectively (equations 9 and 10):

TABLE 2 Measured intracellular metabolite concentrations under N-limited chemostat cultivation of *S. cerevisiae* ($D = 0.05\ h^{-1}$)

Metabolite	Concn[a] (mmol/liter$_{IC}$)		
	NH_4^+	Urea	Glutamate
Ammonium	3.2 ± 1.1	3.8 ± 0.3	3.8 ± 1.2
Urea	BQL	0.151 ± 0.083	BQL
Glutamate	39.4 ± 1.3	36.4 ± 4.2	80.5 ± 5.9
Glutamine	14.1 ± 0.6	13.1 ± 1.6	15. 3 ± 0.9
Alanine	18.8 ± 0.6	16.6 ± 2.3	21.4 ± 1.4
Pyruvate	3.6 ± 0.2	3.7 ± 0.7	2.9 ± 0.2
αKG	0.33 ± 0.01	0.52 ± 0.06	3.07 ± 0.05
NAD	0.82 ± 0.09	0.92 ± 0.08	1.18 ± 0.12
NADH	0.01 ± 0.01	0.02 ± 0.01	0.05 ± 0.03
NADP	0.21 ± 0.03	0.24 ± 0.01	0.22 ± 0.02
NADPH	0.02 ± 0.01	0.02 ± 0.00	0.02 ± 0.00
AMP	0.29 ± 0.03	0.33 ± 0.03	0.38 ± 0.04
ADP	0.69 ± 0.02	0.78 ± 0.04	0.97 ± 0.04
ATP	2.2 ± 0.1	2.3 ± 0.1	2.8 ± 0.1

[a] D is equal to 0.05 h^{-1}. The results shown are averages ± SD of three independent samples from the same steady state. BQL, below the quantification limit. Urea steady-state samples were concentrated twice for higher analytical accuracy; ammonium and glutamate steady-state samples were not measured with larger biomass amounts. The energy charges were 0.80 ± 0.03, 0.79 ± 0.03, and 0.80 ± 0.03 for ammonium, urea, and glutamate, respectively.

$$\frac{[NH_3 + NH_4^+]_{Vac}}{[NH_3 + NH_4^+]_{Cyt}} = \left(\frac{1 + 10^{pK_a - pH_{Vac}}}{1 + 10^{pK_a - pH_{Cyt}}}\right) = 97.2 \quad (9)$$

$$\frac{[NH_3 + NH_4^+]_{Mit}}{[NH_3 + NH_4^+]_{Cyt}} = \left(\frac{1 + 10^{pK_a - pH_{Mit}}}{1 + 10^{pK_a - pH_{Cyt}}}\right) = 0.1 \quad (10)$$

Using a pK_a of 9.25 and a pH_{Vac} of 4.5, it was observed that the vacuole can indeed store a substantial amount of ammonium, but the mitochondrion does not function as an NH_4^+ storage compartment, given its small volume and high pH. (iv) Finally, the kinetic parameters (V_{max} and K_m) for the different transmembrane ammonium transporters were estimated by Marini and coworkers (17, 60). Here, it is assumed that only Mep2 is relevant as the main ammonium transporter, as suggested by previous transcriptomics data obtained from N-limited cultivations (49). The values found were V_{max}, 600 μmol/g_{CDW}/h (equivalent to 20 nmol/min/$mg_{Protein}$ [17], assuming 0.5 $g_{Protein}/g_{CDW}$), and K_m, 2 μmol/liter (17), while the kinetic expression (61) that describes ammonium uptake under N-limiting conditions is as follows:

$$-q_N = -V_{max} \times \left(\frac{[NH_3 + NH_4^+]_{EC}}{[NH_3 + NH_4^+]_{EC} + K_m}\right) \times \left(1 - \frac{\frac{[NH_3 + NH_4^+]_{Cyt}}{[NH_3 + NH_4^+]_{EC}}}{K_{eq}}\right) \quad (11)$$

Equation 11 is a q-linear expression (61) that can be used to model the specific nitrogen source uptake rate ($-q_{N\ source}$) based on the maximum ammonium uptake rate (V_{max}), the thermodynamic driving force $\{1 - Q/K_{eq} = 1 - ([NH_3 + NH_4^+]_{Cyt}/[NH_3 + NH_4^+]_{EC})/K_{eq}\}$ (where Q is the reaction quotient and K_{eq} is the thermodynamic equilibrium constant), and the mechanism-specific nonlinear function of the extracellular concentrations and affinity $\{[NH_3 + NH_4^+]_{EC}/([NH_3 + NH_4^+]_{EC} + K_m)\}$ (K_m) of the main transporter.

Given that $-q_N$ and total intracellular and extracellular ammonium are measured experimentally, the system of four algebraic equations (equations 8 to 11) can be solved using any conventional solver (for instance, fsolve in Matlab) to calculate pH_{Vac}, $[NH_4^+]_{Cyt}$, $[NH_4^+]_{Mit}$, and $[NH_4^+]_{Vac}$. These calculations (Fig. 2B) do indeed show that most of the intracellular ammonium is compartmentalized in the vacuole (around 95% of the total intracellular pool) and that the cytosolic NH_4^+ concentration is very low. This result is consistent with the experimental observations using the analogue molecule methylamine, which suggested that most of the methylamine is compartmentalized (15, 53). Figure 2B also shows that, with the very low $[NH_4^+]_{Cyt}$, the $[NH_4^+]_{Cyt}/[NH_4^+]_{EC}$ ratio is 30, which is about 50% of the thermodynamic equilibrium value for the uniport mechanism. This in turn shows that the NH_4^+

TABLE 3 Experimental Gibbs free energy of reaction ($\Delta_r G'$) of selected central N metabolism reactions in *S. cerevisiae* using whole-cell concentrations

Reaction	Direction	$\Delta_r G'$ (kJ/mol)[a]			Comment[b]
		NH_4^+	Urea	Glutamate	
Gdh1 (cytosolic; NADPH dependent)	L-Glutamate synthesis	−7.4	−8.3	−11.6	Whole cell
		−13.9	−15.6	−18.0	Excluding NH_4^+ compartmentalization
		−7.3	−9.0	−11.5	Compartmentalization (including NH_4^+)
Gdh2 (cytosolic; NADH dependent)	L-Glutamate degradation	+3.0	+4.8	+9.3	Whole cell
		−8.2	−6.5	−4.1	Excluding NH_4^+ compartmentalization
		−14.8	−13.1	−10.7	Compartmentalization (including NH_4^+)
Glutamine synthetase (cytosolic)	L-Glutamate synthesis	−11.1	−11.3	−12.8	Whole cell[c]
		−19.8	−20.0	−21.6	Compartmentalization (including NH_4^+)[c]
GOGAT (cytosolic; NADH dependent)	L-Glutamate synthesis	−26.4	−27.9	−30.8	Whole cell
		−10.6	−11.9	−12.7	Compartmentalization (including NH_4^+)
Alanine aminotransferase	L-Alanine synthesis	−7.8	−7.0	−3.3	Whole cell

[a] Calculations were performed using the online tool eQuilibrator (86, 87); in all cases, pH_{Cyt} was equal to 6.5 and I was equal to 0.25 M.

[b] In cases excluding NH_4^+ compartmentalization, all metabolites except ammonium were considered, compartmentalized as follows: 5% of the total αKG was considered cytosolic ($\alpha KG_{Cyt} = 0.05 \times \alpha KG_{IC}/0.7$), similar to other eukaryotic systems (88); 90% of the glutamate was cytosolic ($Glu_{Cyt} = 0.90 \times Glu_{IC}/0.7$) (88); and 13.6% of the intracellular glutamine was assumed to be cytosolic, based on the thermodynamic equilibrium of the known Gln/H^+ vacuolar antiporters (89). A cytosolic NADPH/NADP ratio of 22 was used, as estimated by Zhang et al. (72); a cytosolic NAD/NADH ratio of 320 was used, as estimated by Canelas et al. (73).

[c] The intracellular phosphate content was assumed to be 106.22 μmol/g_{CDW}, as reported by Zhang et al. (90) for phosphate excess conditions. Cytosolic phosphate was assumed to be 25.02 μmol/g_{CDW} (90), which is the value reported for phosphate excess conditions. The energy of phosphorylation assumed was −45 kJ/mol_{ATP} (91).

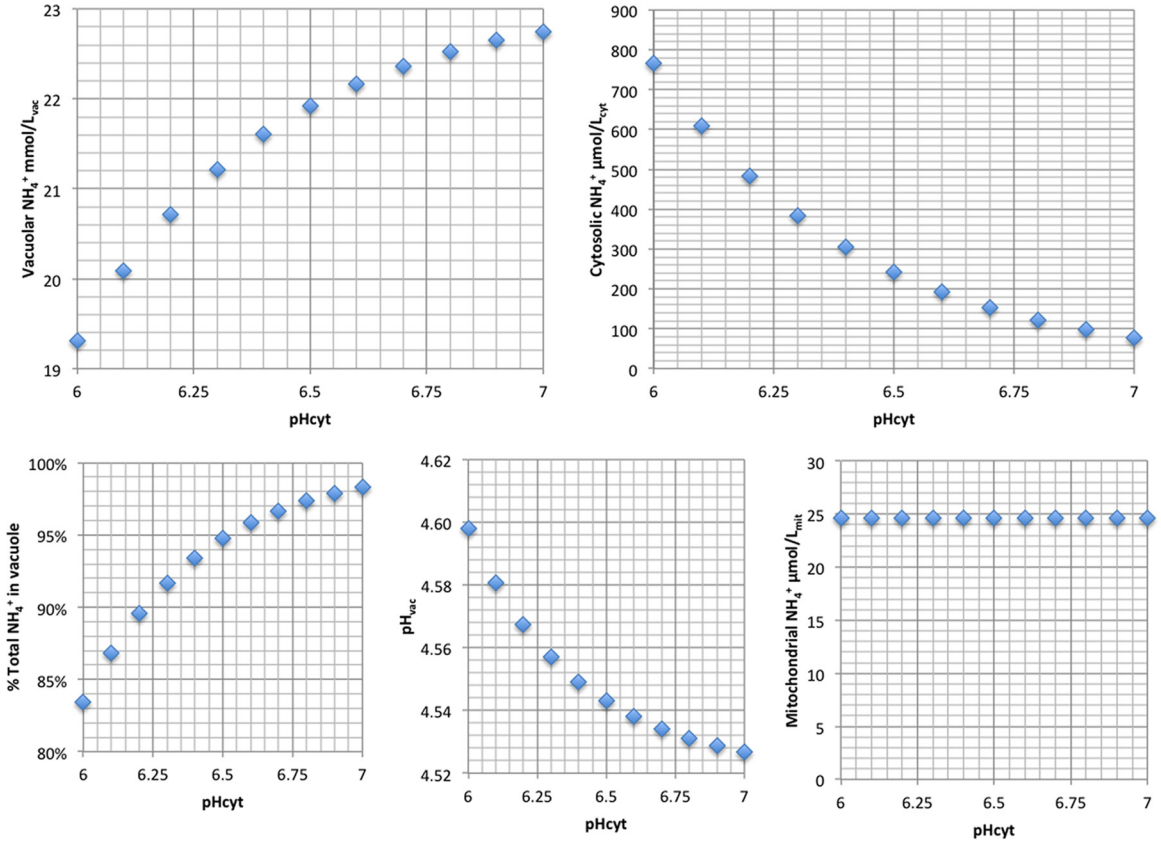

FIG 3 Sensitivity analysis of $[NH_4^+]_{Cyt}$, $[NH_4^+]_{Vac}$, percent total NH_4^+ in the vacuole, pH_{Vac}, and $[NH_4^+]_{Mit}$ values with respect to pH_{Cyt}. The greatest impact was observed in $[NH_4^+]_{Cyt}$ and percent total NH_4^+ in the vacuole, whereas in pH_{Vac} and $[NH_4^+]_{Vac}$, the impact was less than 10%; pH_{Cyt} had no impact on $[NH_4^+]_{Mit}$.

transporter operates not far from thermodynamic equilibrium, if it is an NH_4^+ uniporter or a thermodynamically equivalent mechanism.

The results shown in Fig. 2B depend on the assumption of pH_{Cyt}. Experimental evidence shows that pH_{Vac} could take values between 4 and 5 and pH_{Cyt} is 6 to 7. Figure 3 shows a sensitivity analysis for the effect of pH_{Cyt} on the intracellular ammonium distribution. It can be seen that the previous result, where the majority of NH_4^+ is present in the vacuole, is not very sensitive to the assumed pH_{Cyt}.

Our results show that the cytosolic pool of ammonium has a high turnover rate; given the measured ammonium consumption in this experiment ($-q_N$) of 226 μmol/g_{CDW}/h and the calculated cytosolic ammonium content of 0.345 μmol/g_{CDW}, it is possible to calculate the turnover time of the cytosolic ammonium as on the order of 5.5 s. The turnover time of the entire intracellular ammonium pool will be 20 times longer: 110 s. This short turnover time shows that, for reliable intracellular NH_4^+ measurements, rapid sampling is indeed required.

NH_3/NH_4^+ futile cycling under N limitation in *S. cerevisiae*. From the calculated intracellular ammonium distribution (Fig. 2B), we observed an outward concentration gradient for the neutral species NH_3. This gradient leads to leakage of NH_3 from the intracellular space into the extracellular environment.

Combined with the uptake of NH_4^+, which dissociates into intracellular NH_3 (the species that leaks out of the cell) and H^+, this requires H^+ export by H^+-ATPase, leading to a futile cycle where, for each mole of NH_3 leaked out, there is dissipation of 1 mol ATP. The NH_3 futile-cycling rate follows from the permeability of NH_3 (P_{1a} = 1.73 m/h [6]), the specific cell membrane area (a_m [in square meters] per gram CDW), and the NH_3 concentration difference ($[NH_3]_{Cyt} - [NH_3]_{EC}$) (Fig. 2) as follows:

$$-q_{N_{efflux}} = P_{1a} \times a_m \times ([NH_3]_{cyt} - [NH_3]_{EC}) = \left(1.73\frac{m}{h}\right) \times \left(3.22\frac{m^2}{g_{CDW}}\right) \times \left(402\frac{\mu mol}{m^3} - 0.3\frac{\mu mol}{m^3}\right) = 2{,}236\ \frac{\mu mol}{g_{CDW} \times h} \quad (12)$$

This means that the total Mep-based ammonium influx should equal $-(q_N + q_{Nefflux})$, which is equal to −2,462 μmol/g_{CDW}/h. Most of the studies of NH_4^+ and methylamine transport measured a V_{max} for Mep transporters between 600 and 2,100 μmol/g_{CDW}/h (equivalent to 20 and 70 nmol/min/$mg_{Protein}$ [17], respectively, assuming 0.5 $g_{Protein}/g_{CDW}$). However, the value measured in previous studies has always been the net flux into the cell, which is the real total ammonium uptake rate minus the rate of NH_3 leakage. This implies that the Mep-facilitated transport velocity may have been underestimated at least 2-fold. Every mole of NH_3 leaked out requires a mole of ATP to excrete one H^+ in order to maintain a constant intracellular charge and pH, resulting in an

ATP dissipation rate of about 2.24 mmol ATP/g_{CDW}/h (see equation 12 above).

The extra ATP consumption resulting from the futile cycling of NH_3/NH_4^+ across the cell membrane likely accounts for the extra 4.7 mmol ATP/g_{CDW}/h consumed under N-limited compared to glucose-limited conditions. It is important to note that futile cycling is insignificant under glucose-limiting conditions, where the extracellular NH_4^+ is present at far higher levels than in the cytosol. Furthermore, the inherent leakiness of biological membranes to NH_3 points up an important feature of the vacuole, namely, that eukaryotic cells create and use an acidic compartment to accumulate large amounts of NH_4^+ without a requirement for specific transporters. In the absence of vacuolar compartmentalization, the cytosolic levels of NH_3 could lead to a higher NH_3 efflux rate and enhanced futile cycling, necessitating an increased demand for ATP to maintain proper cytosolic NH_4^+/NH_3 homeostasis.

Wood et al. (15) have derived similar conclusions based on studies with *vma*-deficient yeasts incubated with methylamine.

Urea transport in *S. cerevisiae*. In contrast to the experimental observations for ammonium, the extracellular urea represents a bigger fraction (>80%) of the total broth urea than the intracellular urea. The concentration is higher in the intracellular space (151.3 ± 83.6 μmol/$liter_{IC}$) than in the extracellular space (23.7 ± 9.9 μmol/liter), which indicates active urea transport (Fig. 2B). It was suggested by ElBerry et al. (62) that at low urea concentrations, a special urea transporter (Dur3) is expressed; according to Sanguinetti et al. (63), this urea transporter uses a proton symport mechanism to take up urea, and it is expressed when the extracellular concentrations of urea are below 0.25 mM (62). The expected equilibrium Cyt/EC ratio of urea for this type of transporter is expressed mathematically as follows:

$$\frac{[\text{Urea}]_{\text{Cyt}}}{[\text{Urea}]_{\text{EC}}} = \exp\left(\frac{z \times F \times \text{pmf}}{R \times T}\right) = 2{,}117 \qquad (13)$$

In this case, z is equal to +1 (symport of urea plus one proton) and PMF is equal to 200 mV. Thus, the equilibrium Cyt/EC ratio is 2,117. There are no reports of urea being compartmentalized in *S. cerevisiae*, so it is assumed that all intracellular urea is found in the cytosol. Experimentally, the urea concentration ratio was 6, and the $[\text{urea}]_{\text{Cyt}}/[\text{urea}]_{\text{EC}}$ ratio was equal to 6/0.7, which is equal to 9; unlike the ammonium transporter, the urea symporter is working at far from equilibrium conditions ($Q/K\text{eq} \approx 0.004$). The cytosolic urea concentration (0.15/0.7 = 0.21 mM) is close to the reported K_m value for the urea amidolyase reaction (0.1 and 0.39 mM [64]) and allophanate hydrolase reactions. The high thermodynamic driving force for the urea transporter is probably maintained by high activity of the enzyme urea amidolyase, which quickly metabolizes the intracellular urea.

L-Glutamate transport in *S. cerevisiae*. Glutamate and glutamine are the central metabolites of nitrogen metabolism in yeast. Any other amino acid can be synthesized from these two by means of various reactions, usually involving transaminases (65). Amino acids control the expression of their specific transporters; in the case of glutamate, there are specific dicarboxylic acid permeases (65), particularly Dip5 (66). In the presence of poor nitrogen sources or nitrogen limitation, however, most of these specific permeases are replaced by general amino acid permeases (1); for instance, Gap1 is derepressed under nitrogen-limited conditions (49, 67). There is a general consensus that amino acid permeases work using an electrochemical gradient, by means of H^+ symport (2, 68). Various widely used genome scale stoichiometric models (23–25) assume that the cotransported amino acid species is the zero-charged species in the case of neutral amino acids, the −1 species for acidic amino acids, and the +1 species for basic amino acids; for the particular case of glutamate, however, early experimental evidence from Cockburn et al. (69) showed that glutamate uptake requires cotransport of 2 mol of H^+ per mol of glutamate.

From our experimental results (Fig. 2B), the IC/EC ratio equals 180. Because glutamate is reported not to be strongly compartmentalized and is expected to be mainly cytosolic (70), the Cyt/EC ratio (180/0.7 = 221) follows. This ratio corresponds to a Glu^0/H^+ symport, which has an equilibrium Cyt/EC ratio of 6,017 (see Fig. S1 in the supplemental material), in agreement with the experimental findings of Cockburn et al. (69) but not with the generally assumed Glu^-/H^+ symport (Cyt/EC ratio = 28) (23–25). This suggests that, under glutamate limitation, a different, more active transport is present. However, a Glu^0/H^+ symport mechanism yields a higher Cyt/EC ratio at the cost of ATP expenditure higher than that of Glu^-/H^+ symport. Based on our proteomics analysis, we hypothesize that Agp1, which is known to transport neutral amino acids (71), could be the transporter used by yeast to take up Glu^0, together with one H^+.

Thermodynamic state of central N metabolism reactions. The thermodynamic analysis of the central N metabolism also reinforces the hypothesis of NH_4^+ compartmentalization. When the whole-cell metabolite amounts are used to calculate $\Delta_r G'$ for the glutamate dehydrogenase NADH-dependent (Gdh2) reaction, the values indicate that the reaction is unfeasible toward glutamate conversion into NH_4^+, even when glutamate is used as the N source. Given that Gdh2 is arguably the main source of intracellular NH_4^+ when cells grow using L-glutamate as the N source, the estimation of $\Delta_r G'$ using whole-cell amounts is in conflict with experimental evidence. On the other hand, when metabolite compartmentalization is considered, $\Delta_r G'$ for Gdh2 becomes negative, so the reaction is feasible. In this case, it is assumed that NH_4^+, glutamate, αKG (this study), NADP/NADPH (72), and NAD/NADH (73) are compartmentalized. This results in higher concentrations of substrates than of products, leading to a negative $\Delta_r G'$.

Additionally, the GS-GOGAT system is far from equilibrium, favoring the direction of glutamate production. Our thermodynamic analysis of the central N metabolism points to the possible presence of some futile redox cycles generating unnecessary waste of ATP, for instance, glutamate synthesis by the NADPH-dependent enzyme Gdh1 (K_m for ammonium, 10 mM [64]) and concomitant glutamate degradation by Gdh2 (NAD dependent). Because both enzymes were expressed under ammonium-limited conditions (49), as observed in the proteomics results (see Data Set S1 in the supplemental material), this evidence also supports previous reports of a necessary tight control of the expression of the enzymes involved in the central N metabolism (65).

Protein abundance under different N sources. Our proteomic analysis revealed N source-dependent differences in the abundances and sets of proteins identified, indicating that N-limited growth does not result in a common proteome composition. In cells grown using urea as the sole N source, more than 150 proteins (>3 confidence peptides) that were not found in cells grown using the other two N sources were identified. Among the unique set of urea-specific proteins were Crh1, Dur1 and -2, Dur3,

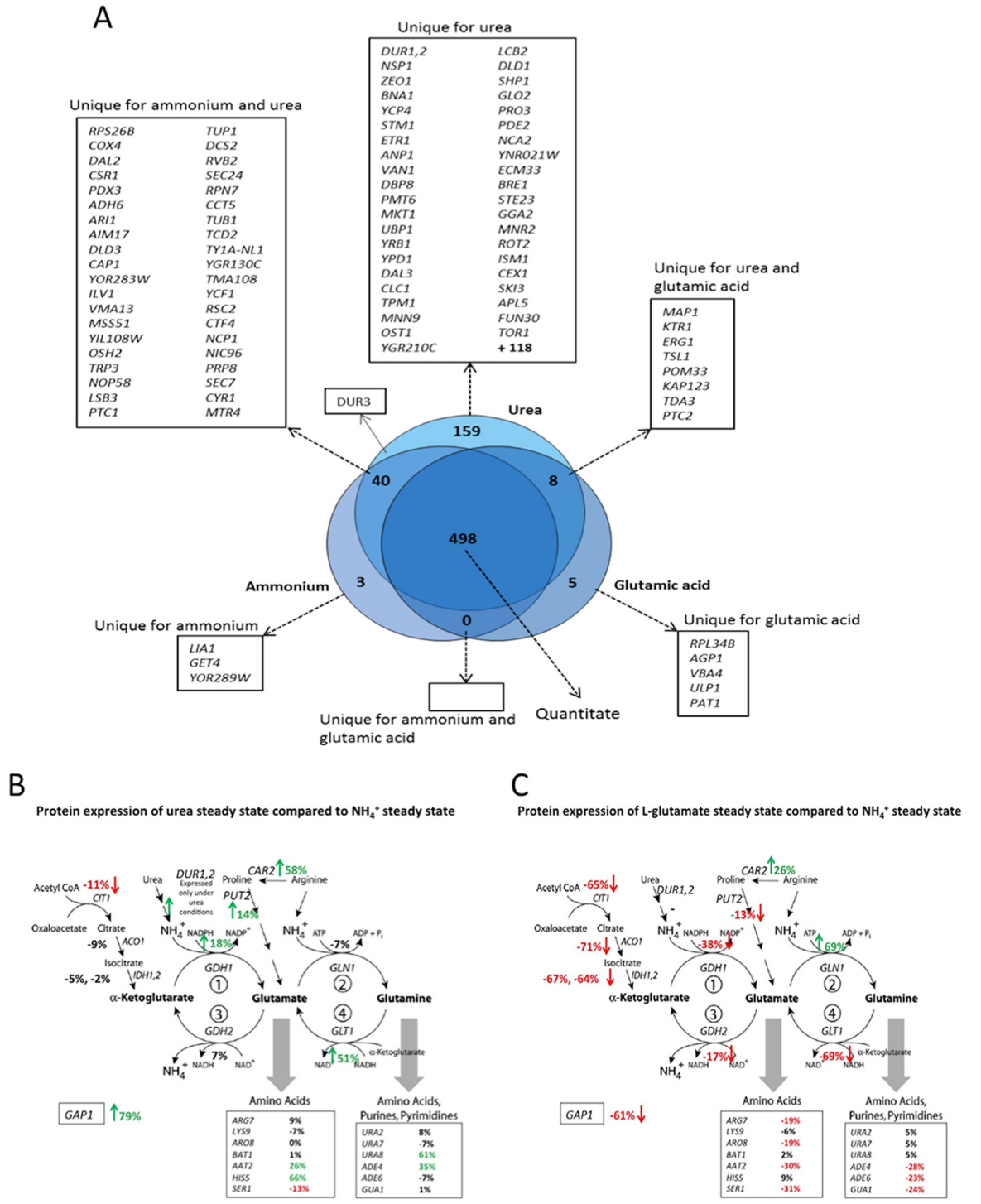

FIG 4 (A) Summary of the large proteomic survey for *S. cerevisiae* at steady state ($D = 0.05\ h^{-1}$) under aerobic N-limiting conditions using different N sources. In this study, it is considered that unique proteins are those proteins that have an expression level high enough to be identified with 3 or more confidence peptides but not identified under other environmental conditions. (B and C) Comparison of protein expression patterns between urea and ammonium steady states (B) and glutamate and ammonium steady states (C). Overexpressed proteins are highlighted in green, repressed proteins are shown in red, and proteins with no changes in expression pattern (<10% difference with respect to the reference steady state) are displayed in black.

Dal5, and Dal8. The higher levels of Crh1 are consistent with previous transcriptomics analysis (3): Crh1 expression is enhanced in urea-grown cells. The Dur and Dal genes, which encode proteins related to urea and allantoin metabolism, are known to be nitrogen regulated and consequently not repressed during growth on urea (74). Also, consistent with urea being a nonrepressive N source, levels of Gap1, Car2, and Glt1 were higher by >50% than in NH_4^+-grown cells (Fig. 4B).

Interestingly, other urea-specific proteins found in our analysis include Tor1, Npr1, and Ure2, proteins required for proper control of NCR-regulated gene expression (1, 2, 75). Based on previous findings, in urea-grown cells, Npr1 and Ure2 should not be (hyper)phosphorylated (1, 76, 77) and the Tor1 kinase is expected to be inactive (1, 78). Consequently, our finding these proteins only in urea-grown cells was presumably due to the experimental procedure used; apparently, phosphorylation interferes with the proper identification of peptides derived from these proteins in cells grown using glutamate or NH_4^+. An alternative experimental protocol, e.g., TiO_2-based separation of phosphoproteins, will be required to identify and quantify proteins with posttranslational modifications (79).

Agp1 and Vba1 were among the five proteins uniquely found in glutamate-grown cells. Agp1 encodes a low-affinity broad-substrate-range amino acid permease that is expressed under the control of the SPS amino acid sensing system (71, 80–82). The higher levels of Agp1 are consistent with transcriptomic analysis (3); in comparison to urea- or NH_4^+-grown cells, Agp1expression is induced. Little is known regarding Vba4 function and expression (74), but it is thought to function as a basic amino acid transporter localized to the vacuolar membrane (83).

We also observed a major shift in the levels of carbon metabolism-related proteins. This is likely due to glutamate, in addition to being an N source, being consumed as a C source. Consistent with previous reports (3, 75), we found that the levels of several proteins of the tricarboxylic acid (TCA) cycle, such as Cit1, Aco1, and Idh1 and -2, were low. So, too, the levels of key enzymes of the central nitrogen metabolism, Gdh2 and Glt1, were low. In the case of Glt1, it is known that its expression is repressed during growth on glutamate (84); glutamate does not need to be synthesized when it is supplied in the medium.

When glutamate is the sole N source, the rest of the amino acids are synthesized using transamination reactions and ammonium is needed only for glutamine synthesis, so Gdh2 is necessary as the main intracellular ammonium-producing reaction. The expression of Gdh2 is regulated by many factors, including the intracellular ammonium concentration and NCR (3, 75), and it is particularly sensitive to the presence of ammonium under batch conditions (75) but upregulated under N limitation (85). It is expected, then, that overexpression of Gdh2 means higher enzymatic activity and hence higher intracellular ammonium concentrations when glutamate is the N source. We therefore hypothesize that the repression of Gdh2 is related to intracellular ammonium homeostasis to avoid accumulation of large quantities of intracellular ammonium, perhaps by means of a feedback inhibition mechanism.

Conclusions. Our experimental measurements suggest that, in aerobic NH_4^+-limited cultivations, most (about 85%) of the ammonium is found in the intracellular space. This result fits with the hypothesis of ammonium transport by means of Mep proteins using a uniport mechanism or with an equivalent thermodynamic equilibrium constant that maintains a high intracellular ammonium concentration even at low ammonium concentrations in the extracellular space. Furthermore, the experimentally measured extracellular concentrations are consistent with previous reports about the capacity and affinity of ammonium transporters (Mep proteins) (17), indicating that at low ammonium concentrations the most active transporter is Mep2, with an affinity constant between 1 μmol/liter and 2 μmol/liter. Under the experimental conditions, it is expected that Mep1 and Mep3 will also be present, but given their kinetic properties (17) and optimal pH (14), their contribution to total ammonium uptake will be lower than that of Mep2. The experiments under aerobic N source limitation using urea and glutamate suggest that these compounds are transported using a proton symport mechanism. In the case of glutamate, the experimental data are consistent with Glu^0 (the uncharged form) symport. Our observations are in agreement with previous experimental findings from Cockburn et al. (69), who suggested that glutamate (Glu^-) is cotransported with 2 mol of H^+ per mol of glutamate taken up.

For the tested N sources, the intracellular and extracellular ammonium concentrations were similar, with a mean total intracellular concentration of 3.6 $mmol/liter_{IC}$ and an extracellular concentration of 8 $\mu mol/liter_{EC}$. These results indicate that there is a minimum amount of ammonium required to regulate and drive the important reactions related to N metabolism and that this concentration has a major effect on the expression of key proteins of the central nitrogen metabolism, as observed in the case of Gdh2 repression during the glutamate steady state.

The experimental results also suggest that there is very significant vacuolar/cytosol compartmentalization of NH_4^+ in *S. cerevisiae*, observed consistently for the three N sources used. Furthermore, the extracellular ammonium concentration suggests the presence of a futile cycle due to NH_3 leakage under aerobic N-limited conditions. According to our estimations, this futile cycle could cost the cells as much as 30% of the total ATP produced.

Finally, it was observed that most of the main central N metabolism reactions were found to be far from equilibrium, which suggests that thermodynamic assumptions, such as the equilibrium of glutamate dehydrogenase NADPH-dependent reactions, cannot be used to study NH_4^+ metabolism in *S. cerevisiae*.

ACKNOWLEDGMENTS

We thank Pascale Daran-Lapujade, Marijke Luttik, and Tim Vos for the use of the Coulter counter equipment for cell volume and particle size distribution measurements and Nick Milne, Jean-Marc Daran, and A. J. A. van Maris for their valuable collaboration and fruitful discussions. H.F.C.-R. thanks the entire CSE group for help during rapid-sampling experiments, and particularly Camilo Suárez-Méndez, Cristina Bernal, Mihir Shah, Leonor Guedes da Silva, Mariana Velasco-Álvarez, and Francisca Lameiras for their invaluable help and collaboration.

This project is sponsored by the BE-BASIC Foundation. H.F.C.-R. thanks CONACyT for a scholarship.

FUNDING INFORMATION

This work, including the efforts of Hugo Federico Cueto-Rojas, Reza Maleki Seifar, Angela ten Pierick, Ward van Helmond, Mervin Pieterse, Joseph J. Heijnen, and S. A. Wahl, was funded by BE-BASIC. This work, including the efforts of Hugo Federico Cueto-Rojas, was funded by Consejo Nacional de Ciencia y Tecnología (CONACYT) (212059).

The funders had no role in study design, data collection and interpretation, or the decision to submit the work for publication.

REFERENCES

1. **Conrad M, Schothorst J, Kankipati HN, Van Zeebroeck G, Rubio-Texeira M, Thevelein JM.** 2014. Nutrient sensing and signaling in the yeast *Saccharomyces cerevisiae*. FEMS Microbiol Rev **38:**254–299. http://dx.doi.org/10.1111/1574-6976.12065.
2. **Ljungdahl PO, Daignan-Fornier B.** 2012. Regulation of amino acid, nucleotide, and phosphate metabolism in *Saccharomyces cerevisiae*. Genetics **190:**885–929. http://dx.doi.org/10.1534/genetics.111.133306.

3. **Godard P, Urrestarazu A, Vissers S, Kontos K, Bontempi G, van Helden J, Andre B.** 2007. Effect of 21 different nitrogen sources on global gene expression in the yeast Saccharomyces cerevisiae. Mol Cell Biol **27:**3065–3086. http://dx.doi.org/10.1128/MCB.01084-06.
4. **Winkler FK.** 2006. Amt/MEP/Rh proteins conduct ammonia. Pflugers Arch **451:**701–707. http://dx.doi.org/10.1007/s00424-005-1511-6.
5. **Kleiner D.** 1981. The transport of NH_3 and HN_4^+ across biological membranes. Biochim Biophys Acta **639:**41–52. http://dx.doi.org/10.1016/0304-4173(81)90004-5.
6. **Antonenko YN, Pohl P, Denisov GA.** 1997. Permeation of ammonia across bilayer lipid membranes studied by ammonium ion selective microelectrodes. Biophys J **72:**2187–2195. http://dx.doi.org/10.1016/S0006-3495(97)78862-3.
7. **Labotka RJ, Lundberg P, Kuchel PW.** 1995. Ammonia permeability of erythrocyte membrane studied by ^{14}N and ^{15}N saturation transfer NMR spectroscopy. Am J Physiol **268:**C686–C699.
8. **Khademi S, O'Connell J, Remis J, Robles-Colmenares Y, Miericke LJW, Stroud RM.** 2004. Mechanism of ammonia transport by Amt/MEP/Rh: structure of *AmtB* at 1.3.5 angstrom. Science **305:**1587–1594. http://dx.doi.org/10.1126/science.1101952.
9. **Gruswitz F, Chaudhary S, Ho JD, Schlessinger A, Pezeshki B, Ho CM, Sali A, Westhoff CM, Stroud RM.** 2010. Function of human Rh based on structure of RhCG at 2.1 A. Proc Natl Acad Sci U S A **107:**9638–9643. http://dx.doi.org/10.1073/pnas.1003587107.
10. **Javelle A, Lupo D, Li X-D, Merrick M, Chami M, Ripoche P, Winkler FK.** 2007. Reprint of "Structural and mechanistic aspects of Amt/Rh proteins" [J Struct Biol. 158 (2007) 472-481]. J Struct Biol **159:**243–252. http://dx.doi.org/10.1016/S1047-8477(07)00165-7.
11. **Nakhoul NL, Lee Hamm L.** 2013. Characteristics of mammalian Rh glycoproteins (SLC42 transporters) and their role in acid-base transport. Mol Aspects Med **34:**629–637. http://dx.doi.org/10.1016/j.mam.2012.05.013.
12. **Hess DC, Lu W, Rabinowitz JD, Botstein D.** 2006. Ammonium toxicity and potassium limitation in yeast. PLoS Biol **4:**e351. http://dx.doi.org/10.1371/journal.pbio.0040351.
13. **Van Nuland A, Vandormael P, Donaton M, Alenquer M, Lourenco A, Quintino E, Versele M, Thevelein JM.** 2006. Ammonium permease-based sensing mechanism for rapid ammonium activation of the protein kinase A pathway in yeast. Mol Microbiol **59:**1485–1505. http://dx.doi.org/10.1111/j.1365-2958.2005.05043.x.
14. **Boeckstaens M, Andre B, Marini AM.** 2008. Distinct transport mechanisms in yeast ammonium transport/sensor proteins of the Mep/Amt/Rh family and impact on filamentation. J Biol Chem **283:**21362–21370. http://dx.doi.org/10.1074/jbc.M801467200.
15. **Wood CC, Poree F, Dreyer I, Koehler GJ, Udvardi MK.** 2006. Mechanisms of ammonium transport, accumulation, and retention in oocytes and yeast cells expressing Arabidopsis *AtAMT1;1*. FEBS Lett **580:**3931–3936. http://dx.doi.org/10.1016/j.febslet.2006.06.026.
16. **Ullmann RT, Andrade SL, Ullmann GM.** 2012. Thermodynamics of transport through the ammonium transporter *Amt-1* investigated with free energy calculations. J Phys Chem B **116:**9690–9703. http://dx.doi.org/10.1021/jp305440f.
17. **Marini AM, Soussi-Boudekou S, Vissers S, Andre B.** 1997. A family of ammonium transporters in *Saccharomyces cerevisiae*. Mol Cell Biol **17:**4282–4293. http://dx.doi.org/10.1128/MCB.17.8.4282.
18. **Crepin L, Sanchez I, Nidelet T, Dequin S, Camarasa C.** 2014. Efficient ammonium uptake and mobilization of vacuolar arginine by *Saccharomyces cerevisiae* wine strains during wine fermentation. Microb Cell Fact **13:**109. http://dx.doi.org/10.1186/s12934-014-0109-0.
19. **Mortimer RK.** 2000. Evolution and variation of the yeast (Saccharomyces) genome. Genome Res **10:**403–409. http://dx.doi.org/10.1101/gr.10.4.403.
20. **Cooper TG, Sumrada R.** 1975. Urea transport in *Saccharomyces cerevisiae*. J Bacteriol **121:**571–576.
21. **Abreu C, Sanguinetti M, Amillis S, Ramon A.** 2010. UreA, the major urea/H^+ symporter in *Aspergillus nidulans*. Fungal Genet Biol **47:**1023–1033. http://dx.doi.org/10.1016/j.fgb.2010.07.004.
22. **Milne N, Luttik MA, Cueto Rojas HF, Wahl A, van Maris AJ, Pronk JT, Daran JM.** 2015. Functional expression of a heterologous nickel-dependent, ATP-independent urease in *Saccharomyces cerevisiae*. Metab Eng **30:**130–140. http://dx.doi.org/10.1016/j.ymben.2015.05.003.
23. **Duarte NC, Herrgard MJ, Palsson BO.** 2004. Reconstruction and validation of Saccharomyces cerevisiae iND750, a fully compartmentalized genome-scale metabolic model. Genome Res **14:**1298–1309. http://dx.doi.org/10.1101/gr.2250904.
24. **Herrgard MJ, Swainston N, Dobson P, Dunn WB, Arga KY, Arvas M, Bluthgen N, Borger S, Costenoble R, Heinemann M, Hucka M, Le Novere N, Li P, Liebermeister W, Mo ML, Oliveira AP, Petranovic D, Pettifer S, Simeonidis E, Smallbone K, Spasic I, Weichart D, Brent R, Broomhead DS, Westerhoff HV, Kirdar B, Penttila M, Klipp E, Palsson BO, Sauer U, Oliver SG, Mendes P, Nielsen J, Kell DB.** 2008. A consensus yeast metabolic network reconstruction obtained from a community approach to systems biology. Nat Biotechnol **26:**1155–1160. http://dx.doi.org/10.1038/nbt1492.
25. **Nookaew I, Jewett MC, Meechai A, Thammarongtham C, Laoteng K, Cheevadhanarak S, Nielsen J, Bhumiratana S.** 2008. The genome-scale metabolic model iIN800 of Saccharomyces cerevisiae and its validation: a scaffold to query lipid metabolism. BMC Syst Biol **2:**71. http://dx.doi.org/10.1186/1752-0509-2-71.
26. **Magasanik B.** 2003. Ammonia assimilation by *Saccharomyces cerevisiae*. Eukaryot Cell **2:**827–829. http://dx.doi.org/10.1128/EC.2.5.827-829.2003.
27. **Magasanik B, Kaiser CA.** 2002. Nitrogen regulation in *Saccharomyces cerevisiae*. Gene **290:**1–18. http://dx.doi.org/10.1016/S0378-1119(02)00558-9.
28. **Dikicioglu D, Karabekmez E, Rash B, Pir P, Kirdar B, Oliver SG.** 2011. How yeast re-programmes its transcriptional profile in response to different nutrient impulses. BMC Syst Biol **5:**148. http://dx.doi.org/10.1186/1752-0509-5-148.
29. **Fayyad-Kazan M, Feller A, Bodo E, Boeckstaens M, Marini AM, Dubois E, Georis I.** 2016. Yeast nitrogen catabolite repression is sustained by signals distinct from glutamine and glutamate reservoirs. Mol Microbiol **99:**360–379. http://dx.doi.org/10.1111/mmi.13236.
30. **de Jonge LP, Buijs NA, ten Pierick A, Deshmukh A, Zhao Z, Kiel JA, Heijnen JJ, van Gulik WM.** 2011. Scale-down of penicillin production in *Penicillium chrysogenum*. Biotechnol J **6:**944–958. http://dx.doi.org/10.1002/biot.201000409.
31. **Cueto-Rojas H, Maleki Seifar R, ten Pierick A, Heijnen S, Wahl A.** 2016. Accurate measurement of the in vivo ammonium concentration in Saccharomyces cerevisiae. Metabolites **6:**12. http://dx.doi.org/10.3390/metabo6020012.
32. **Boer VM, de Winde JH, Pronk JT, Piper MD.** 2003. The genome-wide transcriptional responses of *Saccharomyces cerevisiae* grown on glucose in aerobic chemostat cultures limited for carbon, nitrogen, phosphorus, or sulfur. J Biol Chem **278:**3265–3274. http://dx.doi.org/10.1074/jbc.M209759200.
33. **Silverman SJ, Petti AA, Slavov N, Parsons L, Briehof R, Thiberge SY, Zenklusen D, Gandhi SJ, Larson DR, Singer RH, Botstein D.** 2010. Metabolic cycling in single yeast cells from unsynchronized steady-state populations limited on glucose or phosphate. Proc Natl Acad Sci U S A **107:**6946–6951. http://dx.doi.org/10.1073/pnas.1002422107.
34. **Suarez-Mendez CA, Hanemaaijer M, ten Pierick A, Wolters JC, Heijnen JJ, Wahl SA.** 2016. Interaction of storage carbohydrates and other cyclic fluxes with central metabolism: a quantitative approach by non-stationary 13C metabolic flux analysis. Metab Eng Commun **3:**52–63. http://dx.doi.org/10.1016/j.meteno.2016.01.001.
35. **Mashego MR, van Gulik WM, Vinke JL, Visser D, Heijnen JJ.** 2006. *In vivo* kinetics with rapid perturbation experiments in *Saccharomyces cerevisiae* using a second-generation BioScope. Metab Eng **8:**370–383. http://dx.doi.org/10.1016/j.ymben.2006.02.002.
36. **Lange HC, Eman M, van Zuijlen G, Visser D, van Dam JC, Frank J, de Mattos MJ, Heijnen JJ.** 2001. Improved rapid sampling for *in vivo* kinetics of intracellular metabolites in *Saccharomyces cerevisiae*. Biotechnol Bioeng **75:**406–415. http://dx.doi.org/10.1002/bit.10048.
37. **Canelas AB, ten Pierick A, Ras C, Maleki Seifar R, van Dam JC, van Gulik WM, Heijnen JJ.** 2009. Quantitative evaluation of intracellular metabolite extraction techniques for yeast metabolomics. Anal Chem **81:**7379–7389. http://dx.doi.org/10.1021/ac900999t.
38. **Bisschops MM, Zwartjens P, Keuter SG, Pronk JT, Daran-Lapujade P.** 2014. To divide or not to divide: a key role of *Rim15* in calorie-restricted yeast cultures. Biochim Biophys Acta **1843:**1020–1030. http://dx.doi.org/10.1016/j.bbamcr.2014.01.026.
39. **Cruz AL, Verbon AJ, Geurink LJ, Verheijen PJ, Heijnen JJ, van Gulik WM.** 2012. Use of sequential-batch fermentations to characterize the impact of mild hypothermic temperatures on the anaerobic stoichiometry and kinetics of *Saccharomyces cerevisiae*. Biotechnol Bioeng **109:**1735–1744. http://dx.doi.org/10.1002/bit.24454.
40. **Niedenfuhr S, Pierick AT, van Dam PT, Suarez-Mendez CA, Noh K,**

Wahl SA. 2016. Natural isotope correction of MS/MS measurements for metabolomics and C fluxomics. Biotechnol Bioeng **113:**1137–1147. http://dx.doi.org/10.1002/bit.25859.

41. **Maleki Seifar R, Ras C, Deshmukh AT, Bekers KM, Suarez-Mendez CA, da Cruz AL, van Gulik WM, Heijnen JJ.** 2013. Quantitative analysis of intracellular coenzymes in *Saccharomyces cerevisiae* using ion pair reversed phase ultra high performance liquid chromatography tandem mass spectrometry. J Chromatogr A **1311:**115–120. http://dx.doi.org/10.1016/j.chroma.2013.08.076.
42. **Maleki Seifar R, Ras C, van Dam JC, van Gulik WM, Heijnen JJ, van Winden WA.** 2009. Simultaneous quantification of free nucleotides in complex biological samples using ion pair reversed phase liquid chromatography isotope dilution tandem mass spectrometry. Anal Biochem **388:** 213–219. http://dx.doi.org/10.1016/j.ab.2009.02.025.
43. **Wu L, Mashego MR, van Dam JC, Proell AM, Vinke JL, Ras C, van Winden WA, van Gulik WM, Heijnen JJ.** 2005. Quantitative analysis of the microbial metabolome by isotope dilution mass spectrometry using uniformly ^{13}C-labeled cell extracts as internal standards. Anal Biochem **336:**164–171. http://dx.doi.org/10.1016/j.ab.2004.09.001.
44. **Meiring HD, van der Heeft E, ten Hove GJ, de Jong APJM.** 2002. Nanoscale LC-MS(n): technical design and applications to peptide and protein analysis. J Sep Sci **25:**557–568. http://dx.doi.org/10.1002/1615-9314(20020601)25:9<557::AID-JSSC557>3.0.CO;2-F.
45. **Finoulst I, Vink P, Rovers E, Pieterse M, Pinkse M, Bos E, Verhaert P.** 2011. Identification of low abundant secreted proteins and peptides from primary culture supernatants of human T-cells. J Proteomics **75:**23–33. http://dx.doi.org/10.1016/j.jprot.2011.03.034.
46. **Mortensen P, Gouw JW, Olsen JV, Ong SE, Rigbolt KT, Bunkenborg J, Cox J, Foster LJ, Heck AJ, Blagoev B, Andersen JS, Mann M.** 2010. MSQuant, an open source platform for mass spectrometry-based quantitative proteomics. J Proteome Res **9:**393–403. http://dx.doi.org/10.1021/pr900721e.
47. **UniProt Consortium.** 2015. UniProt: a hub for protein information. Nucleic Acids Res **43:**D204–D212. http://dx.doi.org/10.1093/nar/gku989.
48. **Boer VM, Crutchfield CA, Bradley PH, Botstein D, Rabinowitz JD.** 2010. Growth-limiting intracellular metabolites in yeast growing under diverse nutrient limitations. Mol Biol Cell **21:**198–211. http://dx.doi.org/10.1091/mbc.E09-07-0597.
49. **Hazelwood LA, Walsh MC, Luttik MA, Daran-Lapujade P, Pronk JT, Daran JM.** 2009. Identity of the growth-limiting nutrient strongly affects storage carbohydrate accumulation in anaerobic chemostat cultures of *Saccharomyces cerevisiae*. Appl Environ Microbiol **75:**6876–6885. http://dx.doi.org/10.1128/AEM.01464-09.
50. **Verduyn C, Stouthamer AH, Scheffers WA, van Dijken JP.** 1991. A theoretical evaluation of growth yields of yeasts. Antonie Van Leeuwenhoek **59:**49–63. http://dx.doi.org/10.1007/BF00582119.
51. **Verduyn C, Postma E, Scheffers WA, van Dijken JP.** 1990. Energetics of *Saccharomyces cerevisiae* in anaerobic glucose-limited chemostat cultures. J Gen Microbiol **136:**405–412. http://dx.doi.org/10.1099/00221287-136-3-405.
52. **Boeckstaens M, Andre B, Marini AM.** 2007. The yeast ammonium transport protein Mep2 and its positive regulator, the Npr1 kinase, play an important role in normal and pseudohyphal growth on various nitrogen media through retrieval of excreted ammonium. Mol Microbiol **64:**534–546. http://dx.doi.org/10.1111/j.1365-2958.2007.05681.x.
53. **Soupene E, Ramirez RM, Kustu S.** 2001. Evidence that fungal MEP proteins mediate diffusion of the uncharged species NH_3 across the cytoplasmic membrane. Mol Cell Biol **21:**5733–5741. http://dx.doi.org/10.1128/MCB.21.17.5733-5741.2001.
54. **Hall JA, Yan D.** 2013. The molecular basis of K^+ exclusion by the *Escherichia coli* ammonium channel *AmtB*. J Biol Chem **288:**14080–14086. http://dx.doi.org/10.1074/jbc.M113.457952.
55. **Ritchie RJ.** 2013. The ammonia transport, retention and futile cycling problem in cyanobacteria. Microb Ecol **65:**180–196. http://dx.doi.org/10.1007/s00248-012-0111-1.
56. **Brett CL, Kallay L, Hua Z, Green R, Chyou A, Zhang Y, Graham TR, Donowitz M, Rao R.** 2011. Genome-wide analysis reveals the vacuolar pH-stat of *Saccharomyces cerevisiae*. PLoS One **6:**e17619. http://dx.doi.org/10.1371/journal.pone.0017619.
57. **Uchida M, Sun Y, McDermott G, Knoechel C, Le Gros MA, Parkinson D, Drubin DG, Larabell CA.** 2011. Quantitative analysis of yeast internal architecture using soft X-ray tomography. Yeast **28:**227–236. http://dx.doi.org/10.1002/yea.1834.
58. **Kresnowati MT, Suarez-Mendez C, Groothuizen MK, van Winden WA, Heijnen JJ.** 2007. Measurement of fast dynamic intracellular pH in *Saccharomyces cerevisiae* using benzoic acid pulse. Biotechnol Bioeng **97:**86–98. http://dx.doi.org/10.1002/bit.21179.
59. **Orij R, Postmus J, Ter Beek A, Brul S, Smits GJ.** 2009. *In vivo* measurement of cytosolic and mitochondrial pH using a pH-sensitive GFP derivative in *Saccharomyces cerevisiae* reveals a relation between intracellular pH and growth. Microbiology **155:**268–278. http://dx.doi.org/10.1099/mic.0.022038-0.
60. **Marini AM, Boeckstaens M, Andre B.** 2006. From yeast ammonium transporters to rhesus proteins, isolation and functional characterization. Transfus Clin Biol **13:**95–96. http://dx.doi.org/10.1016/j.tracli.2006.03.002.
61. **Canelas AB, Ras C, ten Pierick A, van Gulik WM, Heijnen JJ.** 2011. An *in vivo* data-driven framework for classification and quantification of enzyme kinetics and determination of apparent thermodynamic data. Metab Eng **13:**294–306. http://dx.doi.org/10.1016/j.ymben.2011.02.005.
62. **ElBerry HM, Majumdar ML, Cunningham TS, Sumrada RA, Cooper TG.** 1993. Regulation of the urea active transporter gene (DUR3) in *Saccharomyces cerevisiae*. J Bacteriol **175:**4688–4698.
63. **Sanguinetti M, Amillis S, Pantano S, Scazzocchio C, Ramon A.** 2014. Modelling and mutational analysis of *Aspergillus nidulans* UreA, a member of the subfamily of urea/H^+ transporters in fungi and plants. Open Biol **4:**140070. http://dx.doi.org/10.1098/rsob.140070.
64. **Schomburg I, Chang A, Ebeling C, Gremse M, Heldt C, Huhn G, Schomburg D.** 2004. BRENDA, the enzyme database: updates and major new developments. Nucleic Acids Res **32:**D431–D433. http://dx.doi.org/10.1093/nar/gkh081.
65. **Hofman-Bang J.** 1999. Nitrogen catabolite repression in *Saccharomyces cerevisiae*. Mol Biotechnol **12:**35–73. http://dx.doi.org/10.1385/MB:12:1:35.
66. **Regenberg B, Holmberg S, Olsen LD, Kielland-Brandt MC.** 1998. Dip5p mediates high-affinity and high-capacity transport of L-glutamate and L-aspartate in *Saccharomyces cerevisiae*. Curr Genet **33:**171–177. http://dx.doi.org/10.1007/s002940050324.
67. **Chiva R, Baiges I, Mas A, Guillamon JM.** 2009. The role of GAP1 gene in the nitrogen metabolism of *Saccharomyces cerevisiae* during wine fermentation. J Appl Microbiol **107:**235–244. http://dx.doi.org/10.1111/j.1365-2672.2009.04201.x.
68. **Horák J.** 1997. Yeast nutrient transporters. Biochim Biophys Acta **1331:** 41–79. http://dx.doi.org/10.1016/S0304-4157(96)00015-9.
69. **Cockburn M, Earnshaw P, Eddy AA.** 1975. The stoichiometry of the absorption of protons with phosphate and L-glutamate by yeasts of the genus Saccharomyces. Biochem J **146:**705–712. http://dx.doi.org/10.1042/bj1460705.
70. **Ishimoto M, Sugimoto N, Sekito T, Kawano-Kawada M, Kakinuma Y.** 2012. ATP-dependent export of neutral amino acids by vacuolar membrane vesicles of *Saccharomyces cerevisiae*. Biosci Biotechnol Biochem **76:** 1802–1804. http://dx.doi.org/10.1271/bbb.120372.
71. **Iraqui I, Vissers S, Bernard F, de Craene J-O, Boles E, Urrestarazu A, André B.** 1999. Amino acid signaling in *Saccharomyces cerevisiae*: a permease-like sensor of external amino acids and F-box protein Grr1p are required for transcriptional induction of the *AGP1* gene, which encodes a broad-specificity amino acid permease. Mol Cell Biol **19:**989–1001. http://dx.doi.org/10.1128/MCB.19.2.989.
72. **Zhang J, Pierick AT, van Rossum HM, Maleki Seifar R, Ras C, Daran JM, Heijnen JJ, Aljoscha Wahl S.** 2015. Determination of the cytosolic NADPH/NADP ratio in *Saccharomyces cerevisiae* using shikimate dehydrogenase as sensor reaction. Sci Rep **5:**12846. http://dx.doi.org/10.1038/srep12846.
73. **Canelas AB, van Gulik WM, Heijnen JJ.** 2008. Determination of the cytosolic free NAD/NADH ratio in *Saccharomyces cerevisiae* under steady-state and highly dynamic conditions. Biotechnol Bioeng **100:**734–743. http://dx.doi.org/10.1002/bit.21813.
74. **Cherry JM, Hong EL, Amundsen C, Balakrishnan R, Binkley G, Chan ET, Christie KR, Costanzo MC, Dwight SS, Engel SR, Fisk DG, Hirschman JE, Hitz BC, Karra K, Krieger CJ, Miyasato SR, Nash RS, Park J, Skrzypek MS, Simison M, Weng S, Wong ED.** 2012. Saccharomyces Genome Database: the genomics resource of budding yeast. Nucleic Acids Res **40:**D700–D705. http://dx.doi.org/10.1093/nar/gkr1029.
75. **Tate JJ, Cooper TG.** 2003. Tor1/2 regulation of retrograde gene expression in *Saccharomyces cerevisiae* derives indirectly as a consequence of alterations in ammonia metabolism. J Biol Chem **278:**36924–36933. http://dx.doi.org/10.1074/jbc.M301829200.

76. **Schmidt A, Beck T, Koller A, Kunz J, Hall MN.** 1998. The TOR nutrient signalling pathway phosphorylates NPR1 and inhibits turnover of the tryptophan permease. EMBO J **17:**6924–6931. http://dx.doi.org/10.1093/emboj/17.23.6924.
77. **Feller A, Georis I, Tate JJ, Cooper TG, Dubois E.** 2013. Alterations in the Ure2 alphaCap domain elicit different GATA factor responses to rapamycin treatment and nitrogen limitation. J Biol Chem **288:**1841–1855. http://dx.doi.org/10.1074/jbc.M112.385054.
78. **Crespo JL, Hall MN.** 2002. Elucidating TOR signaling and rapamycin action: lessons from Saccharomyces cerevisiae. Microbiol Mol Biol Rev **66:**579–591. http://dx.doi.org/10.1128/MMBR.66.4.579-591.2002.
79. **Pinkse MW, Mohammed S, Gouw JW, van Breukelen B, Vos HR, Heck AJ.** 2008. Highly robust, automated, and sensitive online TiO2-based phosphoproteomics applied to study endogenous phosphorylation in Drosophila melanogaster. J Proteome Res **7:**687–697. http://dx.doi.org/10.1021/pr700605z.
80. **Schreve JL, Sin JK, Garrett JM.** 1998. The *Saccharomyces cerevisiae YCC5*(*YCL025c*) gene encodes an amino acid permease, Agp1, which transports asparagine and glutamine. J Bacteriol **180:**2556–2559.
81. **Liu Z, Thornton J, Spirek M, Butow RA.** 2008. Activation of the SPS amino acid-sensing pathway in Saccharomyces cerevisiae correlates with the phosphorylation state of a sensor component, Ptr3. Mol Cell Biol **28:**551–563. http://dx.doi.org/10.1128/MCB.00929-07.
82. **Omnus DJ, Ljungdahl PO.** 2013. Rts1-protein phosphatase 2A antagonizes Ptr3-mediated activation of the signaling protease Ssy5 by casein kinase I. Mol Biol Cell **24:**1480–1492. http://dx.doi.org/10.1091/mbc.E13-01-0019.
83. **Shimazu M, Sekito T, Akiyama K, Ohsumi Y, Kakinuma Y.** 2005. A family of basic amino acid transporters of the vacuolar membrane from *Saccharomyces cerevisiae*. J Biol Chem **280:**4851–4857. http://dx.doi.org/10.1074/jbc.M412617200.
84. **Valenzuela L, Ballario P, Aranda C, Filetici P, Gonzalez A.** 1998. Regulation of expression of *GLT1*, the gene encoding glutamate synthase in *Saccharomyces cerevisiae*. J Bacteriol **180:**3533–3540.
85. **Barbosa C, Garcia-Martinez J, Perez-Ortin JE, Mendes-Ferreira A.** 2015. Comparative transcriptomic analysis reveals similarities and dissimilarities in Saccharomyces cerevisiae wine strains response to nitrogen availability. PLoS One **10:**e0122709. http://dx.doi.org/10.1371/journal.pone.0122709.
86. **Noor E, Haraldsdottir HS, Milo R, Fleming RM.** 2013. Consistent estimation of Gibbs energy using component contributions. PLoS Comput Biol **9:**e1003098. http://dx.doi.org/10.1371/journal.pcbi.1003098.
87. **Noor E, Bar-Even A, Flamholz A, Lubling Y, Davidi D, Milo R.** 2012. An integrated open framework for thermodynamics of reactions that combines accuracy and coverage. Bioinformatics **28:**2037–2044. http://dx.doi.org/10.1093/bioinformatics/bts317.
88. **Lu M, Zhou L, Stanley WC, Cabrera ME, Saidel GM, Yu X.** 2008. Role of the malate-aspartate shuttle on the metabolic response to myocardial ischemia. J Theor Biol **254:**466–475. http://dx.doi.org/10.1016/j.jtbi.2008.05.033.
89. **Sekito T, Fujiki Y, Ohsumi Y, Kakinuma Y.** 2008. Novel families of vacuolar amino acid transporters. IUBMB Life **60:**519–525. http://dx.doi.org/10.1002/iub.92.
90. **Zhang J, Sassen T, ten Pierick A, Ras C, Heijnen JJ, Wahl SA.** 2015. A fast sensor for *in vivo* quantification of cytosolic phosphate in *Saccharomyces cerevisiae*. Biotechnol Bioeng **112:**1033–1046. http://dx.doi.org/10.1002/bit.25516.
91. **de Kok S, Kozak BU, Pronk JT, van Maris AJ.** 2012. Energy coupling in *Saccharomyces cerevisiae*: selected opportunities for metabolic engineering. FEMS Yeast Res **12:**387–397. http://dx.doi.org/10.1111/j.1567-1364.2012.00799.x.